



Tracing the role of Arctic shelf processes in Si and N cycling and export through the Fram Strait: Insights from combined silicon and nitrate isotopes

Margot C.F. Debyser¹, Laetitia Pichevin¹, Robyn E. Tuerena², Paul A. Dodd³, Antonia Doncila¹, Raja S. Ganeshram¹

¹School of Geosciences, University of Edinburgh, Edinburgh, EH9 3FE, United Kingdom

²Scottish Association for Marine Science, Dunstaffnage, PA37 1QA, United Kingdom

³Norwegian Polar Institute, Tromsø, 9296, Norway

Correspondence to: Margot C.F. Debyser (margot.debyser@ed.ac.uk)

Abstract. Nutrient cycles in the Arctic ocean are being altered by changing hydrography, increasing riverine inputs, glacial melt and sea-ice loss due to climate change. In this study, combined isotopic measurements of dissolved nitrate ($\delta^{15}\text{N-NO}_3$ and $\delta^{18}\text{O-NO}_3$) and silicon ($\delta^{30}\text{Si(OH)}_4$) are used to understand the pathways that major nutrients follow through the Arctic ocean. Atlantic waters were found to be isotopically lighter ($\delta^{30}\text{Si(OH)}_4 = 1.74\text{‰}$) than their polar counterpart ($\delta^{30}\text{Si(OH)}_4 = 1.85\text{‰}$) owing to partial biological utilisation of dissolved Si (DSi) within the Arctic ocean. Coupled partial benthic denitrification and nitrification on Eurasian Arctic shelves leads to the enrichment of $\delta^{15}\text{N-NO}_3$ and lighter $\delta^{18}\text{O-NO}_3$ in the polar surface waters ($\delta^{15}\text{N-NO}_3 = 5.44\text{‰}$, $\delta^{18}\text{O-NO}_3 = 1.22\text{‰}$) relative to Atlantic waters ($\delta^{15}\text{N-NO}_3 = 5.18\text{‰}$, $\delta^{18}\text{O-NO}_3 = 2.33\text{‰}$). Using a pan-Arctic DSi isotope dataset we find that the input of isotopically light $\delta^{30}\text{Si(OH)}_4$ by Arctic rivers and the subsequent partial biological uptake and biogenic Si burial on Eurasian shelves are the key processes that generate the enriched isotopic signatures of DSi exported through Fram Strait. A similar analysis of $\delta^{15}\text{N-NO}_3$ highlights the role of N-limitation due to denitrification losses on Arctic shelves in generating the excess dissolved silica exported from the Arctic ocean. We estimate that about a third of the dissolved silica exported through Fram Strait is of riverine origin. As the Arctic ocean is N-limited and riverine sources of DSi are increasing faster than nitrogen inputs, a larger export through the Fram Strait is expected in the future. Arctic riverine inputs therefore have the potential to modify the North Atlantic DSi budget and are expected to become more important than variable Pacific and glacial DSi sources over the coming decades.

1 Introduction

The dissolved macronutrients nitrate (NO_3^-) and silicic acid (Si(OH)_4) are key nutrients in sustaining marine primary production in the Arctic ocean, and have distinct sources from the Atlantic and Pacific Oceans (Tremblay et al., 2015). Additionally, river and coastal erosion contribute dissolved silica (DSi) and nitrate which fuel approximately 30% of Arctic-wide net primary productivity (Terhaar et al., 2021). The Greenland Ice Sheet has also been suggested as an important source



30 of DSi to the Arctic ocean (Hatton et al., 2019; Hawkings et al., 2017). It has been estimated that >85% of DSi from riverine sources is not consumed by phytoplankton (Le Fouest et al., 2013) and is exported out instead, but the controlling processes of this remain unclear. Thus, an integrated understanding of the relative importance of sources to the internal cycling of DSi and the controls on the export of DSi to the North Atlantic is lacking. Stable isotope measurements of nitrate ($\delta^{15}\text{N-NO}_3$ & $\delta^{18}\text{O-NO}_3$) and dissolved silica ($\delta^{30}\text{Si(OH)}_4$) can provide useful insights into nutrient sources and cycling within the ocean
35 (Brzezinski et al., 2021; Sigman et al., 2000; Varela et al., 2016), particularly when both isotopes are combined (Grasse et al., 2016; De Souza et al., 2012). In this study, we present the first full profiles of $\delta^{30}\text{Si(OH)}_4$ measurements in Fram Strait and over the East Greenland shelf in conjunction with nitrate isotopes to examine the controls on DSi export through Fram Strait and suggest potential future scenarios.

40 In the Arctic ocean, primary production is controlled by complex interactions between light availability and nutrient limitation (Popova et al., 2012; Yool et al., 2015) which are highly variable both spatially and temporally. Nitrogen is the primary limiting nutrient for primary production in the Arctic (Krisch et al., 2020; Tuerena et al., 2021a) and sedimentary denitrification on shallow Arctic shelves play an important role in limiting nitrogen availability (Fripiat et al. 2018; Granger et al. 2018) making the Arctic ocean a net sink of nitrate overall (Yamamoto-Kawai et al., 2006). In contrast, there is an excess of DSi in the Arctic
45 ocean and a disproportionally large amount of DSi is exported to the North Atlantic via Fram Strait and the Canadian Arctic Archipelago. Budget estimates have shown that the Arctic ocean contributes more than 10% of the DSi entering the North Atlantic (Torres-Valdés et al., 2013).

The net export of DSi from the Arctic ocean is attributed to Pacific water, which enters the Arctic through the Bering Strait,
50 but also freshwater sources, as highlighted in Figure 1. The Arctic ocean receives a disproportionally large volume of freshwater relative to its area (>10% of the world's riverine discharge) from several of the world's largest rivers, such as the Ob, Yenisei, Lena and Kolyma rivers which discharge onto the Eurasian shelves. These four rivers alone provide 1755 km^3 of freshwater to Arctic shelves annually, along with $135 \times 10^9 \text{ g}$ of nitrate and $4816 \times 10^9 \text{ g}$ of DSi (Holmes et al., 2012), which fuels coastal and Arctic-wide productivity, subsequently transported through the Transpolar Drift (TPD) (Terhaar et al., 2021).
55 Arctic glacial meltwaters provide a potentially significant contribution to the Arctic's nutrient budget (Hatton et al., 2019), with DSi and amorphous silica inputs from the Greenland Ice sheet estimated to constitute around 37% of riverine fluxes in the coastal regions of Arctic Seas (Hawkings et al., 2017). However, the fraction that is exported from Greenland and Svalbard fjords into the open ocean is poorly documented.

60 Atlantification is leading to changes in sea-ice cover and stratification of the Eurasian basin (Arthun et al., 2012; Lind et al., 2018) and increasing nutrient availability in the surface ocean (Randelhoff et al., 2018; Tuerena et al., 2021a). Meanwhile, DSi concentrations from Atlantic Waters (AW) are decreasing in the sub-Arctic regions (Hátún et al., 2017) and the inflow of Pacific water is increasing (Woodgate, 2018). Riverine freshwater inputs have been increasing in the Eurasian sector



(McClelland et al., 2006) and nutrient fluxes are increasing in rivers with degrading permafrost (Frey et al., 2007; Frey and
65 McClelland, 2009; Zhang et al., 2021). All of these changes have widespread impact on phytoplankton dynamics (Ardyna and
Arrigo, 2020). In response, the nutrient budgets of the Arctic ocean are expected to change, with potential repercussions on
downstream ecosystems and Atlantic nutrient budgets. In order to predict such impacts, a better understanding of the relative
importance of Arctic nutrient sources and internal cycling is needed.

70 Fram Strait is both an inflow and outflow gateway and a key area of exchange between the Arctic and the North Atlantic. On
the Eastern side, warm, saline AW originating from the subpolar and subtropical gyre of the North Atlantic flows northward
in the surface intensified West Spitsbergen Current. On the Western side, Polar Surface Water (PSW) carries cold, fresh Arctic-
originating water and sea-ice into the Subpolar North Atlantic Ocean in the upper (ca. 250m) part of the water column (Dodd
et al., 2012; Rudels et al., 2002; de Steur et al., 2009). PSW is relatively low in nitrate, carrying the signal of Pacific nutrient
75 stoichiometry and benthic denitrification to the Atlantic Ocean through low N:P ratio (Dodd et al., 2012). In contrast to PSW,
AW has relatively high nitrate concentrations but is poor in DSi ($\cong 5\mu\text{M}$) as this key nutrient is depleted in the Atlantic through
uptake by silicifying phytoplankton species during its northward movement. The stoichiometry of DSi availability compared
to nitrate ($\text{DSi:N} < 1$) in AW in Fram Strait suggests phytoplankton blooms experience DSi limitation prior to nitrate limitation
(Krause et al., 2018, 2019; Tuerena et al., 2021a).

80

Nitrate removal processes within the Arctic ocean are reflected in the nitrate isotopic signatures of 5.5‰ for $\delta^{15}\text{N-NO}_3$ and
1.3‰ for $\delta^{18}\text{O-NO}_3$ of PSW (Tuerena et al., 2021a), which are significantly different from incoming AW signatures of 5.1‰
for $\delta^{15}\text{N-NO}_3$ and 2.4‰ for $\delta^{18}\text{O-NO}_3$. The difference between these two water masses reflects benthic denitrification on
shallow Eurasian shelves, also termed coupled partial nitrification-denitrification (CPND), which increases $\delta^{15}\text{N-NO}_3$ while
85 decreasing $\delta^{18}\text{O-NO}_3$ producing an associated increase in the parameter $\Delta(15-18)$, defined as $\delta^{15}\text{N-NO}_3 - \delta^{18}\text{O-NO}_3$, through
the release of isotopically heavy ammonia from sediments (Fripiat et al. 2011; Granger et al. 2018). PSW transports high DSi
concentrations from Pacific and riverine influence: $\delta^{30}\text{Si(OH)}_4$ of Pacific water is $\cong 1.4\text{‰}$ (Reynolds et al. 2006). This is lighter
than North Atlantic signatures ($\delta^{30}\text{Si(OH)}_4 \cong 1.7\text{‰}$) which are enriched to a greater extent from the Southern Ocean source
signal as DSi is depleted through partial uptake and subsequent burial of DSi in the North Atlantic (Brzezinski and Jones,
90 2015; De Souza et al., 2012). Siberian rivers have high seasonal and regional variability in their isotopic signatures, which are
isotopically low, where $\delta^{30}\text{Si(OH)}_4 = 0.86\text{--}1.08\text{‰}$ (Pokrovsky et al., 2013; Sun et al., 2018) from weathering processes in
Arctic rivers, leading to fractionation of the isotope from the local bedrock. While Arctic sources of DSi are isotopically low,
the Arctic halocline and drift waters are isotopically high ($\delta^{30}\text{Si(OH)}_4 \cong 1.8\text{‰}$), with isotopically heavy deep basins
(Brzezinski et al., 2021; Varela et al., 2016). This is attributed to water mass mixing (Liguori et al., 2020) and biological
95 modification of Atlantic & Pacific water (Varela et al., 2016). A recent study however highlights the importance of biological
productivity and biogenic Si burial of riverine DSi in generating these enriched Arctic signatures (Brzezinski et al., 2021).



Although isotopic signatures have been measured up to 60°N in the Atlantic Ocean (De Souza et al., 2012; Sutton et al., 2018), no direct measurements of $\delta^{30}\text{Si}(\text{OH})_4$ are available from Atlantic-Arctic Gateways such as the Fram Strait. Therefore, $\delta^{30}\text{Si}(\text{OH})_4$ signatures of modified inflowing AW in the Arctic ocean and outflowing PSW and the contributions from East Greenland shelves are unknown.

This study fills this crucial gap in the Arctic silicon isoscape, documenting isotope signatures and nutrient cycling processes in Fram Strait, focussing on the upper water masses. We use a combination of geochemical parameters ($\delta^{30}\text{Si}(\text{OH})_4$, $\delta^{15}\text{N-NO}_3$, $\delta^{18}\text{O-NO}_3$, $\Delta(15-18)$, N^* & Si^*) alongside hydrographic data (salinity, temperature, mixed layer depth) to explore the sources and internal cycling of DSi in the water masses exported through the Fram Strait. We then proceed to put these in the context of pan-Arctic isotope datasets and evaluate the implications of Arctic nutrient cycling on how nutrient export is likely to change in the future with ongoing climate change.

2 Method

2.1 Sample collection

Samples were collected on four CTD sections across the Fram Strait between 2017-2019 (Table 1). The CTD package was equipped with a SBE911plus CTD system recording multiple parameters (conductivity, temperature, pressure & salinity). Salinity was calibrated on-board using an Autosol 8400B salinometer (JR17005) and a Guildline Portasal salinometer (FS2017-2019). Samples for dissolved inorganic nutrient analysis were collected from Niskin bottles and stored in pre-cleaned HDPE bottles which were frozen at -20 °C immediately after collection. Samples for isotopic analysis were filtered inline using Nuclepor polycarbonate membranes (0.4µM porosity) into acid-cleaned polypropylene bottles and stored at -20°C (nitrate isotopes) or acidified at 0.1% v/v with 12M HCl and stored at 4°C (silicon isotopes).

2.2 Dissolved inorganic nutrient measurements

Dissolved inorganic nutrient concentrations for all cruises were determined from frozen samples on autoanalysers following standard colorimetric methods on a Bran and Luebbe QuAAtro 5-channel autoanalyser at the National Oceanographic Centre, UK (JR17005) and on a SmartChem 200 discrete analyser at the Technical University of Denmark (FS2017-19) and calibrated using OSIL nutrient standards.

2.3 Nitrate isotope analysis

$\delta^{15}\text{N-NO}_3$ & $\delta^{18}\text{O-NO}_3$ were measured using the bacterial strain of *P. aureofaciens* following the denitrifier method (Casciotti et al., 2002; Sigman et al., 2001). Measurements were corrected using international reference standards IAEA-N3 and USGS-34 in each run, as well as an internal standard of North Atlantic Deep Water ($\delta^{15}\text{N-NO}_3 = 4.92 \pm 0.12 \text{ ‰}$, $\delta^{18}\text{O-NO}_3 = 1.88 \pm$



0.45‰) for inter-run comparability, with standard reproducibility across runs of $\pm 0.1\text{‰}$ and $\pm 0.4\text{‰}$ for $\delta^{15}\text{N-NO}_3$ & $\delta^{18}\text{O-NO}_3$ respectively. Final values were corrected using the correction scheme described in Weigand et al. (2016) and following Tuerena et al. (2021a, 2021b) for inter-comparability of datasets in the Atlantic-Arctic region.

2.4 Silicon isotope analysis

- 130 As DSi concentrations are very low in the Arctic ocean ($<10\mu\text{M}$), previous protocols from Brzezinski et al. (2003) and Reynolds et al. (2006), originally based on the Magnesium Induced Coprecipitation (MAGIC) method described in Karl and Tien (1992), did not yield high enough Si concentrations post-precipitation for accurate analysis. This method was further optimised to allow measurements at concentrations below $10\mu\text{M}$, and to increase the sensitivity and reproducibility of measurements in the very low concentration range.
- 135 Briefly, a two-step preconcentration was performed on all samples prior to purification. pH of 40ml of sample was increased twice using 400 μL of 1M NaOH to completely scavenge DSi through brucite formation. Precipitates were recovered by centrifugation, re-dissolved using twice-distilled 6M HCl, regrouped and diluted to 2ppm Si with MQ water. The solution was further purified by loading 0.5ml of the solution onto pre-cleaned 1.8ml Biorad AG50W-X8 cation-exchange resin columns and eluted with 3ml of MQ purified water.
- 140 The $\delta^{29}\text{Si(OH)}_4$ composition of the prepared solution was determined by MC-ICP-MS on a Nu Plasma II instrument at the University of Edinburgh using standard-sample bracketing and calculated from the permil deviation from isotopic reference material NBS28 (Georg et al., 2006), calculated as:

$$\delta^{29}\text{Si} = \left(\frac{\left(\frac{^{29}\text{Si}}{^{28}\text{Si}} \right)_{\text{sample}}}{\left(\frac{^{29}\text{Si}}{^{28}\text{Si}} \right)_{\text{NBS28}}} - 1 \right) \times 1000[\text{‰}]$$

- 145 Due to the low DSi concentrations and high salt matrix effects from increased precipitation volumes, interference on the $\delta^{30}\text{Si}$ increased measurement error, and as per Fripiat et al. (2011a, 2011b), $\delta^{29}\text{Si}$ were converted to $\delta^{30}\text{Si}$ for better accuracy and global comparability of datasets (Cardinal et al., 2003, 2005), using the theoretical conversion factor of 1.96, calculated from the kinetic fractionation law (Young et al., 2002).

- Inter-run comparability & method reproducibility of measurements was checked with the international solid standard Big Batch & both high and low concentration seawater standards Aloha₁₀₀₀ & Aloha₃₀₀. Average standard measurements for the period of this study is Aloha₁₀₀₀ = $0.67 \pm 0.03\text{‰}$, $1.32 \pm 0.06\text{‰}$ (n=16), BigBatch = $-5.33 \pm 0.02\text{‰}$, $-10.50 \pm 0.04\text{‰}$ (n=7) for $\delta^{29}\text{Si(OH)}_4$ and $\delta^{30}\text{Si(OH)}_4$ respectively. Long-term reproducibility of converted $\delta^{30}\text{Si(OH)}_4$ is BigBatch = $-10.49 \pm 0.09\text{‰}$ (n=58), Aloha₁₀₀₀ = $1.29 \pm 0.08\text{‰}$ (n=58) and Aloha₃₀₀ = $1.70 \pm 0.05\text{‰}$ (n=30) compared to inter-laboratory measurements of BigBatch = $-10.48 \pm 0.2\text{‰}$, Aloha₁₀₀₀ = $1.25 \pm 0.2\text{‰}$, Aloha₃₀₀ = $1.66 \pm 0.35\text{‰}$ (Grasse et al., 2017; Reynolds et al., 2007).



155 2.5 Derived parameters

Mixed-Layer Depth (MLD) is identified as the maximum depth at which the potential density was within 0.1kgm^{-3} of the shallowest measurement (Peralta-Ferriz and Woodgate, 2015). MLD governs the depth for which nutrients resupply surface waters and to which planktons are mixed (Yool et al., 2015). In this study, PSW is defined as potential temperature (θ) $<0^\circ\text{C}$ and potential density (σ_θ) $<27.7\text{kgm}^{-3}$, and AW is defined as $\theta >2^\circ\text{C}$ and $27.7 < \sigma_\theta < 27.97\text{kgm}^{-3}$ or $\sigma_\theta < 27.7\text{kgm}^{-3}$ and salinity $>34.92\text{psu}$, as per Richter, Von Appen and Wekerle (2018).

The semi-conservative tracers N^* & Si^* were calculated from inorganic nutrient concentrations where $\text{N}^* = \text{NO}_x - \text{PO}_4 \times 16$, adapted from Gruber & Sarmiento (1997), and $\text{Si}^* = \text{DSi} - \text{NO}_x$ (Sarmiento et al., 2004). Both tracers are indicative of nutrient deviation from typical Redfield ratio, and highlight additional sources or processes through which nutrient become deficit (i.e. Negative N^* shows nitrate deficit in comparison to phosphate). The isotopic parameter $\Delta(15-18)$ is calculated as $\Delta(15-18) = \delta^{15}\text{N}-\text{NO}_3 - \delta^{18}\text{O}-\text{NO}_3$. $\Delta(15-18)$ captures variation in both isotopes, tracing sources and modification of nitrate (Rafter et al., 2013).

3 Results

3.1 Hydrography & mixed layer depth

Figure 2 shows temperature and salinity across Fram Strait in July-August 2018. The hydrographic situation is typical of the late summer season. Warm inflowing and recirculating sub-tropical originating AW is found primarily between 2.5°W and the Eastern end of the section at 10°E , in the upper 500 m. Its core flows northward within the West Spitsbergen Current at $6-8^\circ\text{E}$. Over the East Greenland Shelf, PSW dominates the upper 150m, extending from the western end of the section to the AW/PSW interface at about 3°W . Re-circulating Atlantic Waters (RAW), underlays PSW on the East Greenland shelf, while Arctic Atlantic Water (AAW) is also found below AW at the foot of the East Greenland Shelf. We refer the reader to Rudels et al. (2002) for an overview of the properties of watermasses found in Fram Strait.

The MLD did not exceed 100m for FS2018. Late-season MLD was deeper in AW than in PSW, occurring between 30-60m. MLD is significantly shallower over the East Greenland shelf, occurring at 5-10m. Hydrography and nutrient distribution of JR17005 follow roughly similar patterns as FS2018 apart from seasonal variations, and are previously described in Tuerena et al. (2021).

180 3.2 Nutrient concentrations

Panels a and b of Figure 3 show the nitrate and DSi concentrations along the late-summer 2018 Fram Strait section. Nitrate concentrations were low across the section in the upper 50m of the water column from phytoplankton utilisation and dilution by low-nitrate freshwater sources. Below the mixed-layer depth, NO_x is higher in AW (12.10 ± 0.97) than in PSW ($8.24 \pm 2.18\text{ }\mu\text{M}$), consistent with export of low nitrate waters from the Central Arctic.



185 Negative N^* reflecting a deficit of nitrate are evident on the East Greenland Shelf. In contrast, N^* reaches near positive values in AW with an average of -0.55 below the MLD (Table 2). This highlights that nitrate is more depleted in PSW relative to dissolved phosphate, becoming potentially limiting to primary production towards the end of the biological growth season as nitrate concentrations approach $0\mu\text{M}$.

DSi concentrations were low across the section above the MLD, with stronger depletion at shallower depths and further West. 190 Comparison of DSi concentrations measured during May-June 2018 and August-September 2018 (Table 2) reveals that DSi concentrations were higher in PSW ($4.27\mu\text{M}$) than in AW ($3.19\mu\text{M}$) in the mixed layer at the start of the season, but fell to similar concentrations by the end of the summer ($1.03\mu\text{M}$ and $1.26\mu\text{M}$ for AW and PSW respectively).

Below the mixed layer, DSi is lower in AW ($5.42 \pm 0.70 \mu\text{M}$) than in PSW ($6.65 \pm 1.67 \mu\text{M}$), reflecting the import of low-DSi waters Atlantic waters from sub-tropical origins, and export of Arctic-originating waters enriched through various 195 terrestrial, glacial or Pacific sources. In the deep Fram Strait, DSi concentrations vary locally, but generally increase with depth up to a concentration of $9.45\mu\text{M}$ in deep waters (Figure 4). Strongly negative Si^* in AW reflect the strong DSi deficit relative to nitrate in Atlantic-originating waters, while Si^* closer to phytoplankton requirement in PSW illustrate excess DSi in PSW.

3.3 Isotopic measurements

Measured profiles of $\delta^{30}\text{Si}(\text{OH})_4$ across Fram Strait are shown in panel h of Figure 3 and Figure 4. Positive signatures of 200 $\delta^{30}\text{Si}(\text{OH})_4$ were measured throughout the water column, ranging from 1.34‰ to 3.16‰ for the entire section. The heaviest $\delta^{30}\text{Si}(\text{OH})_4$ signatures were measured in the upper 100m of the section, consistent with fractionation from diatom uptake during growth. Below the MLD, mean $\delta^{30}\text{Si}(\text{OH})_4$ for AW was $1.74 \pm 0.06\text{‰}$ (Table 2), which aligns closely with measurements of waters from North Atlantic origin (Brzezinski and Jones, 2015; De Souza et al., 2012). Conversely, DSi in PSW was isotopically heavier than DSi in AW, the mean $\delta^{30}\text{Si}(\text{OH})_4$ value for PSW was $1.87 \pm 0.10\text{‰}$. This is comparable to 205 measurements of the upper halocline layer in the Canadian basin ($\delta^{30}\text{Si}(\text{OH})_4 = 1.84\text{‰}$) from Varela et al. (2016), and outflowing surface measurements from Brzezinski et al. (2021) in the TPD where $\delta^{30}\text{Si}(\text{OH})_4 = 1.92\text{‰}$, and aligns with the heavy signatures of Arctic-originating waters in the North Atlantic (De Souza et al., 2012; Sutton et al., 2018).

In the deep waters of Fram Strait, $\delta^{30}\text{Si}(\text{OH})_4$ are lighter than PSW, aligning with the gradient decrease of 0.15‰ over the full depth profile reported in Brzezinski et al. (2021). The measured signatures also align with measurements in the North Atlantic 210 of Nordic originating endmembers ($\text{DW-}\delta^{30}\text{Si}(\text{OH})_4 = 1.65 \pm 0.13\text{‰}$ & $\text{DSOW-}\delta^{30}\text{Si}(\text{OH})_4 = 1.75 \pm 0.09\text{‰}$, De Souza et al., 2012). Light $\delta^{30}\text{Si}(\text{OH})_4$ values were measured at the sediment interface (Figure 4), showing potential interaction of benthic efflux of DSi from isotopically light pore-waters (Ehlert et al., 2016), and remineralisation of isotopically lighter biogenic Si in the deep. This is also observed in Brzezinski et al. (2021) and Liguori et al. (2020) who found isotopically light measurements in the deep Nansen & Amundsen basins. The strong influence of local circulation precludes quantification of 215 such local recycling processes from advective signals in Fram Strait with certainty.



Figure 5 displays the full water column profiles of nitrate isotopes measured along the spring (JR17005) and late-summer (FS2018) sections. $\delta^{15}\text{N-NO}_3$ is enriched in PSW (5.44‰) compared to AW (5.18‰) while the $\delta^{18}\text{O-NO}_3$ is lighter in PSW (1.22‰) than in AW (2.33‰, Table 2) following trends identified in Tuerena et al. (2021a). The decoupling of both isotopes is reflected in diverging $\Delta(15-18)$, indicative of CPND. A high confidence in accuracy and reproducibility of nitrate isotopes measurements in this study is obtained as the dataset aligns and follow the same trends as profiles reported in Tuerena et al. (2021a).

In surface waters, $\delta^{15}\text{N-NO}_3$ values increase with reducing nitrate concentrations, which is consistent with biological uptake. This is also observed in most $\delta^{18}\text{O-NO}_3$ profiles apart from PSW profiles measured far onto the East Greenland shelf in FS2018 (Figure 3), where signals of denitrification dominates over biological uptake signals, even in the upper water column. As shown in Figure 3, and summarised in Table 2, isotopic signatures of both dissolved silicon and nitrate isotopes closely follow the hydrography of water masses in spring and summer. In Fram Strait, a key area of exchange with the North Atlantic where inflowing & outflowing water masses show strong differences in their physical properties, dissolved nitrate & silicon isotopes measurements provide insights into nutrient sources and cycling within the Arctic ocean and the pathways through which nutrient modification and exchange occurs.

230 4 Discussion

4.1 Using nutrient isotopes to examine Arctic nutrient cycling

4.1.1 Trends between $\delta^{15}\text{N-NO}_3$, $\delta^{30}\text{Si(OH)}_4$ and nutrient utilisation

In this section we compare $\delta^{15}\text{N-NO}_3$ and $\delta^{30}\text{Si(OH)}_4$ measurements with apparent nitrate and DSi utilisation in PSW and AW in Fram Strait in spring and summer 2018 (Figure 6, panels a and b). We define apparent nutrient utilisation as the fraction of nutrient remaining in the surface layer relative to concentrations below the MLD for the watermass. A fraction of 1 indicates no nitrate or DSi has been used, a fraction of 0 indicates complete depletion of the nutrient inventory.

The fractionation of nitrate and DSi during phytoplankton uptake can be described by Rayleigh systematics (Altabet and Francois, 2001; Mariotti et al., 1981), and is often linked to local hydrography. Rayleigh systematics assume a closed system: i.e there is no import/export of the nutrient from the euphotic zone while it is being utilised by phytoplankton. In late spring and summer, the PSW layer in Fram Strait is largely a closed system as it is highly stratified. Nitrate and DSi are mainly replenished during winter destratification (Altabet and Francois, 2001). In this environment, $\delta^{15}\text{N-NO}_3$ and $\delta^{30}\text{Si(OH)}_4$ values can be expected to fall on a trend based on their isotopic effect (~2-6‰ for nitrate and ~1‰ for DSi), and are described by exponential trendlines in the Rayleigh field on Figure 6 (Varela et al., 2004).



In areas of upwelling, or in a case where the resupply of nutrients to the euphotic zone occurs due to multiple stratification and destratification events throughout growth season, the system is better modelled as an open system, described by a linear trendline in the Rayleigh field. However, in low-nutrient zones such as the PSW layer in Fram Strait, nutrient uptake stoichiometry is dictated by nutrient-limitation itself rather than by the physical re-supply of nutrients (Hutchins and Bruland, 1998; Moore et al., 2013), which in turn can lead to a shift from open to closed system dynamics as one nutrient is depleted with respect to other nutrients.

For the spring and summer growth season of 2018, nitrate in AW and PSW enriched in $\delta^{15}\text{N-NO}_3$ at lower nitrate concentrations, consistent with fractionation associated with nutrient uptake by phytoplankton (Figure 6). Two separate closed fractionation lines are shown representing a typical isotopic effect (5‰, red) and a particularly low isotopic effect observed in Tuerena et al. (2021a) for PSW in Fram Strait (2‰, black). Nitrate fractionation in AW followed a linear trend with small fractionation overall, consistent with open system kinetics for spring and summer. This corroborates with the relatively weak stratification of AW (Rudels et al., 2005), facilitating re-supply of nitrate and other nutrients over the spring and summer growth season through destratification events such as those described by Tuerena et al. (2021a).

The relationship between apparent DSi utilisation and $\delta^{30}\text{Si(OH)}_4$ in AW is linear and representative of open-system kinetics throughout the spring and summer growth season (Figure 6) after DSi was drawn down to $1\mu\text{M}$ in AW in summer 2018 (Figure 4). $\delta^{30}\text{Si(OH)}_4$ fractionation in the upper 100m of the water column remained small with no observed fractionation in the Rayleigh field, suggesting complete utilisation and recycling of DSi in the water column. DSi measurements (Figure 4) show that DSi is strongly depleted in surface AW in summer, confirming that DSi is one of the limiting nutrients in AW in the Eastern Fram Strait along with Fe (Krisch et al., 2020). We conclude that changes in $\delta^{30}\text{Si(OH)}_4$ in surface AW in the mixed layer in Fram Strait are controlled by mixing rather than biological processes.

In PSW, a decoupling of the nitrate and DSi systems is observed. As described above, $\delta^{15}\text{N-NO}_3$ fractionation follows an exponential trend and behaves as a closed system in spring, indicative of the strong salinity stratification of PSW, shifting to mostly linear trend in summer, suggesting open system kinematics (Figure 6, panel a and b). However, as PSW is strongly stratified by salinity, it is unlikely the system was open. It is most likely that this change indicates a shift towards consumption of regenerated nitrogen in these nitrate depleted waters.

$\delta^{30}\text{Si(OH)}_4$ in PSW behaves as an open-system in spring but not in summer, shifting towards an exponential trend and Rayleigh kinetics towards the end of the growth season. As all nutrients are equally resupplied during deep mixing, a decoupling in isotopic systems may be indicative of seasonal shifts in nutrient limitation or co-limitation instead. Our results suggest that nitrate is more limiting than DSi in PSW at the start of the season as nitrate is actively drawn down in the highly stratified PSW (closed system). Primary production subsequently shifts towards using regenerated nitrogen, leading to more linear



nitrate utilisation. In contrast to nitrate, biogenic silica is recycled less within the upper water column, as a result the system gets increasingly fractionated over the growth season in the closed system, with increased DSi limitation in PSW.

Nutrient uptake in surface AW is constrained by low DSi concentration throughout the growth season, while uptake in PSW is constrained by strong nitrate limitation at the beginning of the growth season, with partial limitation from DSi at the end of the season. This indicates that DSi uptake is regulated by nitrate availability. $\delta^{15}\text{N-NO}_3$ and $\delta^{30}\text{Si(OH)}_4$ show a strong link between the silicon and nitrogen cycles in Fram Strait as they regulate each other through limitation, contributing to the asymmetry observed in nutrient exports across the strait (Torres-Valdés et al., 2013).

4.1.2 Upstream transformation of nitrate and DSi in PSW and AW in Fram Strait

The nutrient composition of polar waters exported through Fram Strait reflect their nutrient cycling history through altered DSi:N ratio and isotopic signatures. Figure 7a shows trends for $\delta^{15}\text{N-NO}_3$ vs $\delta^{18}\text{O-NO}_3$, displaying that fractionation due to uptake by phytoplankton assimilation follows the established fractionation ratio of 1:1 (Granger et al., 2004; Sigman et al., 2005) but on separate fractionation lines. $\delta^{15}\text{N-NO}_3$ and $\delta^{18}\text{O-NO}_3$ of PSW plots on a fractionation line consistent with isotopically lighter sources of $\delta^{18}\text{O-NO}_3$, while $\delta^{15}\text{N-NO}_3$ and $\delta^{18}\text{O-NO}_3$ measured in surface AW follow a line consistent with isotopically heavier sources, suggesting different nutrient sources in AW and PSW.

The modification of nitrate in the Arctic ocean is readily apparent when plotting N^* against $\delta^{18}\text{O-NO}_3$ (Figure 7b); as salinity decreases and the influence of Polar-originating waters increases, N^* decreases, indicating a nitrogen deficit in relation to phosphate in PSW. Water samples with lower N^* are accompanied by low $\delta^{18}\text{O-NO}_3$ signatures. This relationship is attributed to CPND in the Arctic ocean (Granger et al., 2011): settling particulate nitrogen from coastal productivity degrades at the sediment interface of the extensive shallow shelves, producing large sources of sedimentary ammonium as the high load of particulate organic nitrogen from coastal productivity degrades at the sediment interface. In shelves where sedimentary denitrification preferentially consumes isotopically-light NO_3 , the NH_4^+ thus released into the water column is isotopically heavy in $\delta^{15}\text{N}$. Subsequently, during nitrification, this benthic efflux of isotopically heavy NH_4^+ is combined with light oxygen isotopes nearing local $\delta^{18}\text{O-H}_2\text{O}$ into the nitrate pool. This decouples the two isotopes by lowering the $\delta^{18}\text{O-NO}_3$ of nitrate overall whilst increasing $\delta^{15}\text{N-NO}_3$.

CPND is a widespread process in Arctic shelves and has been observed in the Chukchi Sea (Brown et al., 2015; Granger et al., 2018) and the East Siberian Sea (Fripiat et al., 2018) and contributes to the observed Arctic-wide nitrogen deficit in relation to phosphate (Torres-Valdés et al., 2013; Yamamoto-Kawai et al., 2006). This shelf-derived signal is exported into the Arctic halocline (Granger et al., 2018) through the TPD, and can be traced in the outflowing water-masses in Fram Strait (Tuerena et al., 2021a), reflecting the impact of shelf processes on PSW nutrient ratios. Thus, the low N^* , low $\delta^{18}\text{O-H}_2\text{O}$ and high $\Delta(15-18)$ signal exported in the PSW is the signature of N loss on Eurasian shelves and the Chukchi Sea.



DSi concentrations in outflowing PSW are 1.2 μM higher and $\delta^{30}\text{Si}(\text{OH})_4$ is isotopically heavier by 0.11‰ relative to inflowing
305 AW (Table 2). Documented Pacific and meteoric sources of DSi are isotopically light (Hawkins et al., 2017; Pokrovsky et
al., 2013; Reynolds et al., 2006; Sun et al., 2018) but DSi behaves non-conservatively across the Arctic ocean. DSi uptake by
phytoplankton in the Arctic ocean and loss due to biogenic Si burial fractionate the upper water column $\delta^{30}\text{Si}(\text{OH})_4$ towards
heavier signatures (Brzezinski et al., 2021; Liguori et al., 2020; Varela et al., 2016).

Varela et al. (2016) suggest the heavy signal observed in the deep Arctic is sourced from intermediate Atlantic-originating
310 waters but we observe no significant enrichment of $\delta^{30}\text{Si}(\text{OH})_4$ in the intermediate water masses of Fram Strait (Figure 3,
Figure 4). Given that the inflowing AWs are already too poor in DSi to contribute to isotopic enrichment, the observed increase
in DSi concentrations may point to riverine DSi sources subject to enrichment due to biogenic si production and burial instead
(Brzezinski et al., 2021) .

As seawater is undersaturated with respect to biogenic Si at all depths in the ocean (Archer et al., 1993), biogenic Si dissolution
315 occurs in the water column and at the sediment-water interface. Upon burial, biogenic Si will continue to dissolve until pore-
waters are saturated (Kamatani, 1982; Nelson et al., 1995). Arctic shelves are characterized by a shallow water column with
relatively high sedimentation rates influenced by river and biogenic fluxes, conditions favourable to reduced biogenic Si
exposure to dissolution, and rapid burial. Therefore, it is expected that Arctic shelf seas are particularly efficient at removing
biogenic Si through opal burial. DSi is only partially utilised in the surface as productivity is limited by N deficit, leading to
320 fractionation. The isotopically lighter biogenic Si is preferentially buried leaving water column $\delta^{30}\text{Si}(\text{OH})_4$ heavy overall. This
contrasts with deep Arctic basins with low productivity and long water residence times which provide opportunities for more
remineralisation in the water column and at the water-sediment interface. This leads to relatively small modification in the
water-column $\delta^{30}\text{Si}(\text{OH})_4$ (Brzezinski et al., 2021; Liguori et al., 2020). The heavy $\delta^{30}\text{Si}(\text{OH})_4$ signatures of PSW thus records
the partial utilisation and the loss of lighter Si through burial in the Arctic shelves.

325 Figure 7c shows the relationship between $\Delta(15-18)$ and $\delta^{30}\text{Si}(\text{OH})_4$ in samples below the MLD which should not be affected
by seasonal biological fractionation. A gradient is observed between AW and PSW, with a gradual increase in $\Delta(15-18)$ from
2‰ to 4‰ as salinity decreases, and an increase in $\delta^{30}\text{Si}(\text{OH})_4$ from 1.7‰ to 2‰, linking the processes of denitrification
(Fripiat et al., 2018; Granger et al., 2011, 2018) and removal of isotopically light DSi sources through biogenic Si burial in the
shelves (Brzezinski et al., 2021; Liguori et al., 2020) contributing to the evolution of the dual isotope signal of PSW. The
330 combination of both CPND and biogenic Si burial indicated by the isotopic signatures of N and DSi can only occur in areas
which receive a direct high influx of terrestrial DSi and hosts CPND, namely, the Bering Sea and Eurasian shelves.

AW entering the Arctic is poor in DSi which limits biological uptake in AW (Agusti et al., 2018; Krause et al., 2018, 2019).
Any excess DSi (e.g from Pacific and shelf waters supplied to AW) will be consumed during the growth season until nitrate is
exhausted. The enrichment of $\delta^{30}\text{Si}(\text{OH})_4$ in Arctic waters (Brzezinski et al., 2021; Liguori et al., 2020; Varela et al., 2016)



335 points towards partial utilisation of DSi, constrained by the availability of nitrate. The combination of supply and use of these nutrients is reflected in panel d of Figure 7, where PSW is distinct from AW with positive Si* (DSi sources from terrestrial runoff, Pacific influence where nitrate is in deficit) and heavy $\delta^{30}\text{Si}(\text{OH})_4$ signatures whereas the relationship with salinity reflects the mixing of these distinct water mass signatures. While AW signals remain clustered, large variability in PSW Si* and isotopic signature highlight the regional variation and complexity of the Si budget around the Arctic ocean (Table 2).

340 In summary, the extent of DSi drawdown is regulated and capped by N-deficit through the availability of nitrogen both locally (Fram Strait) and on an Arctic-wide scale through nitrate deficit. PSW carries the isotopic signals of DSi and N modification within Eurasian shelves through processes such as CPND and partial utilisation of DSi.

4.2 Silicate cycling in the Arctic ocean and sources of silicate exported through Fram Strait

The Arctic exports significant amounts of DSi but not N through Fram Strait (Torres-Valdés et al., 2013). Modification of PSW as a result of shelf processes can be traced across the Arctic simultaneously using N & DSi isotopes (Figure 7c). Here we use $\delta^{30}\text{Si}(\text{OH})_4$ versus $\ln[\text{DSi}]$ plots to examine the pathway of this transformation from DSi sources to Fram strait (Figure 8). A broad negative trendline is observed in Figure 8. Decreasing DSi and heavier $\delta^{30}\text{Si}(\text{OH})_4$ suggest that mixed riverine and Pacific sources of DSi are partially utilised in the Eurasian shelf and transported across the Arctic towards Fram Strait through PSW.

350 4.2.1 The Bering Strait inflow

$\delta^{30}\text{Si}(\text{OH})_4$ in the upper 100m of the water column in the North Pacific is relatively light ($\sim 1.5\text{‰}$), with high DSi concentrations ($\sim 40\mu\text{M}$) (Reynolds et al., 2006). Pacific-originating nutrients are strongly modified in the Bering Strait by riverine input with high Si:N ratio from the Yukon river, by benthic denitrification, and significant biological consumption over the broad shallow shelves in the Bering & Chuchki seas. The combined processes lead to increasing $\delta^{30}\text{Si}(\text{OH})_4$ following biological uptake and fractionation (Brzezinski et al., 2021), merging towards signatures resembling riverine endmembers (Sun et al., 2018). Thus there is no pure Pacific endmember measured in the Bering Strait, and Arctic inflow here has low DSi concentrations relative to the Pacific.

4.2.2 The Eurasian shelf signal

Siberian rivers have isotopically low $\delta^{30}\text{Si}(\text{OH})_4$ from clay mineral weathering (Mavromatis et al., 2016; Pokrovsky et al., 2013; Sun et al., 2018). However, terrestrial DSi input and biological consumption occurs simultaneously on shallow Eurasian shelves. Riverine inputs support one third of the net primary productivity of the Arctic ocean (Terhaar et al., 2021), most of which occurs on the Eurasian shelves (MacDonald et al., 2010). Phytoplankton uptake further reduces DSi concentrations and leads to isotopically heavier $\delta^{30}\text{Si}(\text{OH})_4$. This inference follows Brzezinski et al. (2021), as it is also reflected in the TPD. Thus, in Figure 8, the broad negative trendline from riverine and Pacific sources across the TPD to Fram Strait reflects the



365 progressive depletion of DSi through biological uptake and biogenic Si burial resulting in isotopic enrichment as it travels through the Arctic. Partial DSi utilisation modifies both the Si budget and its isotopic composition. DSi transported from Eurasian shelves through the TDP towards Fram Strait is reflected in isotopically heavy $\delta^{30}\text{Si}(\text{OH})_4$ in PSW which aligns with the broad Rayleigh field in Figure 8.

In Fram Strait, $\delta^{30}\text{Si}(\text{OH})_4$ fractionation involves separate trendlines for AW and PSW. The trend for AW is statistically significant at Fram strait ($R^2 > 0.7$) but shifted downwards indicating a distinct Atlantic source. In contrast, the PSW trendline is shifted upwards from AW towards heavier isotopic values and higher DSi concentrations, following more closely the broader Arctic trends. In addition, larger variability in Si isotope signatures of PSW ($R^2 > 0.3$) at Fram strait reflects the mixing between Arctic and Atlantic source signatures around Fram Strait.

4.2.3 Glacial influence on $\delta^{30}\text{Si}(\text{OH})_4$ exported from the Arctic ocean via Fram Strait

375 Glacial and sea ice inputs have been suggested to significantly impact Arctic silica budgets (Fripiat et al., 2014; Hawkings et al., 2017), this is valuated further in Figure 8. Si inputs from Greenland and Svalbard have been suggested as significant contributors to the Arctic Si budget which is exported through PSW to the North Atlantic (Hatton et al., 2019; Hawkings et al., 2017, 2018), though the glacial freshwater content of PSW at 79°N is relatively small (<13%, Stedmon et al., 2015). Isotopic studies in Greenland and Svalbard glaciers have shown isotopically light signatures with low DSi concentrations
380 (Hatton et al., 2019). In Figure 8, we show that low $\delta^{30}\text{Si}(\text{OH})_4$ signatures from Greenland and Svalbard glacial sources also have low DSi concentrations and do not align in the Rayleigh field with the Arctic trend observed. This suggests Greenland and Svalbard glaciers are not significantly impacting the Si budget of outflowing PSW at Fram Strait. This implies in-situ studies of glacial streams in Greenland may overestimate glacial contribution of silica to Eurasian Arctic nutrient budgets. A possible explanation for this is amorphous phases of silica represent >95% of the total silica flux (Hawkings et al., 2017) and
385 a large fraction of this may be buried in the sediments of Arctic Fjords prior to dissolution, reducing the impact of glacially-sourced DSi.

4.2.4 $\delta^{30}\text{Si}(\text{OH})_4$ of sea ice

Sea ice brine is heavier or equal to surrounding waters $\delta^{30}\text{Si}(\text{OH})_4$ (Fripiat et al., 2007, 2014) and may contribute to the isotopically heavy signature of polar waters (Liguori et al., 2020; Varela et al., 2016). A recent study from Brzezinski et al.
390 (2021) did find direct evidence of such an impact on a basin-wide scale. Here we evaluate the role of sea-ice in influencing Arctic $\delta^{30}\text{Si}(\text{OH})_4$ signatures in a region influenced by brine rejection. In Figure 9, we present hydrography and late-summer profiles of DSi and $\delta^{30}\text{Si}(\text{OH})_4$ collected from Ile-de-France section between 2017-2019 (section location is shown in Figure 1). This area is characterized by perennial sea ice cover (Schneider and Budeus, 1995). A PSW layer extends down to 125m of the water column and is influenced by brine released during winter sea ice formation (Budeus and Schneider, 1995). In the
395 freshwater layer, a small peak in DSi concentration (2-3 μM) is observed at ~40m. The small increase in DSi concentration at



this depth suggests a DSi source from sea ice processes. However, there is no distinct isotopic enrichment (Figure 9) associated with this source. Thus while DSi inputs from sea ice cannot be the reason for enriched $\delta^{30}\text{Si}(\text{OH})_4$ signatures of PSW. This inference is consistent with studies suggesting that sea ice and sea ice brine tend to be relatively low in DSi (Fripiat et al., 2017), with no significant impact on pan-Arctic isotope signatures (Brzezinski et al., 2021).

400 4.2.5 Processes affecting the export of Arctic DSi to the Atlantic Ocean

Figure 8 reveals that DSi exported to the Atlantic in PSW in 2018 was sourced from incomplete utilisation of DSi on Eurasian shelves. This leads to the question as to what limits the complete utilisation of DSi in the Arctic. In Figure 10, we plot $\delta^{15}\text{N}\text{-NO}_3$ versus DSi:N ratios, excluding measurements within the MLD at Fram Strait to remove seasonal uptake trends (this was not applied to measurements in the TPD and shelf seas due to the shallow nature of the water masses). The figure reveals the
405 three mixing components of the Arctic N budget, namely, the very heavy $\delta^{15}\text{N}\text{-NO}_3$ values generated on the the shelves with high Si:N ratios due to removal of light nitrate by CPND; The input of terrestrial riverine N with relatively low $\delta^{15}\text{N}\text{-NO}_3$ signatures ($\delta^{15}\text{N}\text{-NO}_3 = 2.3\text{‰}$, Francis, pers. comm.) with variable but high DSi:N ratios; and Atlantic sources ($\delta^{15}\text{N}\text{-NO}_3 = 4.8\text{‰}$, Tuerena et al., 2015, and DSi:N = 0.6, World Ocean Database, 2013). AW sources become important in Fram strait and contribute to nitrate by mixing across the halocline in basins where AW ply below PSW. Pan-Arctic N isotopic trends,
410 shown in Figure 10, are dominated by mixing of sources rather than fractionation by biological uptake; a striking contrast to the $\delta^{30}\text{Si}(\text{OH})_4$ trend (Figure 8). This is arguably caused by the near-complete utilisation of nitrate on Eurasian shelves and above the halocline, leading to limited overall fractionation from source signatures. This widespread nitrate limitation in the Arctic is attributed to fixed N loss from benthic denitrification on the shallow shelves which constitute approximately 50% of the Arctic ocean area. A significant portion of N loss from denitrification is derived from organic matter from the overlying
415 water column (Mctigue et al., 2016; Tuerena et al., 2021c); leading to a net deficit of N exported out of the Arctic (Torres-Valdés et al., 2013; Yamamoto-Kawai et al., 2006).

Furthermore, Arctic rivers are a larger source of DSi than N (Holmes et al., 2012) and the N supplied is quickly removed in river deltas (Tuerena et al., 2021c). For example, on the Laptev sea shelves, it is estimated that 62-76% of riverine dissolved organic nitrogen is removed within a couple of months by denitrification and biological utilisation (Thibodeau et al., 2017).
420 This is evident from the very low nitrate concentrations in the TPD and high DSi:N ratios ($\sim 5\mu\text{M}$ and 1.8 respectively, Doncila, 2020) which is heavily influenced by riverine inputs and modification over the Eurasian shelves. The near-absence of nitrate in surface waters overall contributes to the higher DSi:N output observed in PSW in Fram Strait. We conclude that incomplete utilisation of DSi in the Arctic ocean and its subsequent export through the Fram Strait is governed largely by widespread N limitation in the Arctic ocean due to the rapid removal of nitrate on the Eurasian shelves.



425 4.2.6 Quantifying terrestrial Si sources at Fram Strait

DSi:N in PSW are variable, but are generally high ($\text{DSi:N}_{\text{PSW}} = 0.90\text{--}1.12$), while the Atlantic marine endmember is low: $\text{DSi:N}_{\text{Atlantic}} = 0.43$. Here we evaluate the riverine contribution of DSi leading to high $\text{DSi:N}_{\text{PSW}}$ while balancing observed DSi concentrations and $\delta^{30}\text{Si}(\text{OH})_4$ signatures.

430 In North Pacific waters, nutrient depletion through biological activity leads to an overall decrease in DSi:N and increase in $\delta^{30}\text{Si}(\text{OH})_4$. Assuming further modification of marine $\delta^{30}\text{Si}(\text{OH})_4$ and DSi:N through the Bering Strait is linear with North Pacific trends, Pacific-originating waters may increase Arctic DSi:N from 0.43 in AW up to 0.78 in PSW. $\text{DSi:N} > 0.78$ must originate from terrestrial riverine sources instead to modify the DSi budget of PSW without also increasing the nitrate inventory accordingly.

435 A coarse estimation of riverine DSi can be calculated assuming that all nutrients with ratio of $\text{DSi:N} \leq 0.78$ are of marine origins in the Arctic. Following this, an excess of 1.2 - 3.4 μM of DSi is present with respect to nitrate in PSW where $\text{DSi:N}_{\text{PSW}} > 1$ ($\text{DSi:N}_{\text{Lena}} = 3.6$; where DSi:N was calculated from Holmes et al., 2021). This constitutes 10-30% of the total DSi exported out of Fram Strait. Based on DSi fluxes estimates from Torres-Valdés et al. (2013), this constitutes $5.7 - 17.1 \times 10^{10}$ mol Si annually delivered through Fram Strait to the North Atlantic. This represents 14-42% of the total measured DSi fluxes originating from pan-Arctic rivers in Holmes et al. (2012), in agreement with estimations from Le Fouest et al. (2013) that
440 >85% of riverine DSi does not get consumed due to nitrogen limitation on the Pan-Arctic scale, and is instead exported out of the Arctic.

5 Future implications

Our results highlight some important connections between nutrient cycling and the control on the exchange of nutrients between the Arctic and the Atlantic Ocean. This study has identified a link between the Arctic N and Si cycles: Nitrogen
445 availability regulates DSi drawdown both locally and on a pan-Arctic scale. The nitrogen deficit is generated by biological Arctic shelf processes such as CPND. This along with riverine inputs controls the excess DSi exported out of the Arctic ocean through gateways such as the Fram Strait. In the changing Arctic ocean, this has far-reaching implications to ecosystems and nutrient budgets as discussed below.

Using $\delta^{30}\text{Si}(\text{OH})_4$ signatures, we have estimated that a significant percentage of DSi exported out through Fram Strait is of
450 riverine origin. Freshwater inputs to the Arctic ocean from the Eurasian sector are expected to increase in response to climate change (McClelland et al., 2006; Rawlins et al., 2010). Increasing riverine discharge and permafrost degradation is accelerating the transport of terrestrial material to Eurasian shelves and likely increasing the export of major nutrients (Zhang et al., 2021). As NO_3^- delivery from rivers is low, riverine sources of DSi are increasing faster than N inputs.

Our study illustrates that biogenic Si production in the Arctic is ultimately limited by NO_3^- availability. Nitrogen is quickly
455 removed in Siberian rivers at low salinities (Sanders et al., 2021; Tuerena et al., 2021c) through benthic denitrification, with



roughly 70% of terrestrial N removed before reaching the seawater endmember (Letscher et al., 2013) depleting N in relation to DSi in the deeper water column. Such rapid N removal implies additional terrestrial NO_3^- inputs are not likely to significantly impact N-availability. Nitrogen deficiency on Arctic shelves is currently limiting DSi consumption to only 14.3% of its net riverine input (Le Fouest et al., 2013). This implies that as terrestrial DSi inputs increase, a larger proportion of terrestrial DSi will remain unutilised and ultimately get transported through the TPD out to Fram Strait. This will increase the export of DSi to the North Atlantic, but also alter the $\delta^{30}\text{Si}(\text{OH})_4$ of PSW which is derived from the partial biological utilisation of DSi. Terrestrial DSi inputs increasing in the future combined with increased N-limitation will reduce the percentage of DSi consumption in the Arctic ocean, leading to lighter isotopic signatures of DSi exported towards the North Atlantic.

Locally, the larger export of DSi through the TPD has implications for nutrient dynamics in Fram Strait. N-limitation is strong in PSW and is predicted to increase in AW (Tuerena et al., 2021a). Increasing primary production in the Arctic shelves as sea ice melts and light availability increases (Arrigo et al., 2008; Arrigo and van Dijken, 2015) will increase N-demand, and further N losses through denitrification which could reduce DSi uptake further and limit net productivity from silicifying species and impact carbon drawdown in Fram Strait. A decline in diatoms and a shift towards smaller phytoplankton assemblages is already observed with warming in Fram Strait (Lalande et al., 2013). Such changes will be accentuated further with N-limitation.

We also recognize there are competing influences on the future nutrient status of the Fram Strait. The higher export of DSi can compensate for decreasing DSi supply through AW to the Arctic ocean resulting from Atlantification (Arthun et al., 2012; Lind et al., 2018) which leads to decreasing DSi concentrations in AW (Hátún et al., 2017). While terrestrial increase in DSi input and reduced utilisation in the Arctic will supersede this signal in PSW over time, this can potentially lead to a decrease in the DSi inventory of intermediate and deep waters of the Arctic ocean influenced by AW, while increasing DSi export out of the Arctic through the PSW.

The far-reaching consequences of the predicted future increases in Arctic DSi export to the North Atlantic imply changes to primary production patterns and DSi concentrations in deep water masses formed here. Waters in the North Atlantic are richer in nitrate than DSi, and available evidence indicate DSi limitation of diatom spring blooms due to limiting concentrations of silicic acid in the region (Henson et al., 2006; Leblanc et al., 2005). This envisioned additional supply of DSi can impact the duration of diatom blooms in the sub-Arctic North Atlantic (Allen et al., 2005), and possibly enhance diatom production with subsequent implications for carbon export to the deep ocean. In longer time scales, this can also increase the preformed DSi inventories in the North Atlantic deep waters, with an impact on the nutrient status of the deep water masses worldwide.

6 Conclusions

Previous understanding of the importance of physical (water-mass mixing) vs biological (production and dissolution) controls in setting $\delta^{30}\text{Si}(\text{OH})_4$ distribution across the Arctic was limited by the lack of direct measurements at major gateways (Brzezinski et al., 2021). This study provides the first full depth profiles of $\delta^{30}\text{Si}(\text{OH})_4$ in Fram Strait, in combination with $\delta^{15}\text{N}\text{-NO}_3$ and $\delta^{18}\text{O}\text{-NO}_3$, closing gaps in the Arctic isoscape and confirming mechanisms of transformation.



Isotopic measurements document the transformation of PSW outflowing through Fram Strait, with isotopic signatures $\Delta(15-18) = 4.22\text{‰}$ and $\delta^{30}\text{Si}(\text{OH})_4 = 1.85\text{‰}$. $\delta^{30}\text{Si}(\text{OH})_4$ is significantly enriched by 0.11‰ in PSW compared to inflowing AW, while $\Delta(15-18)$ is enriched by 1.37‰, showing significant source modification of the nutrients between the inflow and outflow waters.

Further examination of DSi & N isotopes trace nutrient sources and modification processes in PSW primarily to Eurasian shelves: The increase in DSi concentration and enrichment of $\delta^{30}\text{Si}(\text{OH})_4$ is traced to biological uptake of DSi and partial burial of biogenic Si on the shelves, sustained by the high DSi load from Eurasian rivers. Export of DSi out of the Arctic through Fram Strait is ultimately regulated by N-limitation resulting from N-poor input from terrestrial sources combined with efficient removal of N through denitrification on shelves. This is documented in PSW through de-coupling of the oxygen and nitrogen isotopes of nitrate from traditional 1:1 relationship. Glacial influence from Greenland and Svalbard glaciers and Pacific inflow appeared of small influence at Fram Strait in PSW, with riverine sources contributing to ~15-40% of the silica exported out of Fram Strait.

The measurement of DSi & N isotopes provides the first insights into the coupling of the N and Si cycle in the Arctic Ocean. Nitrate limitation during primary production generates excess DSi which is subsequently exported to the North Atlantic. As riverine nutrient sources of DSi are expected to increase faster than N with climate warming, this can enhance N limitation within the Arctic ocean and increase the export of DSi to the North Atlantic ocean.

Funding. This work was supported by a Natural Environment Research Council (NERC) Doctoral Training Partnership grant (NE/L002558/1) and from the ARISE project NE/P006310/1 awarded to Raja S. Ganeshram, part of the Changing Arctic ocean programme, jointly funded by the UKRI NERC and the German Federal Ministry of Education and Research (BMBF).

Data availability. Nutrient (<https://doi.org/10/d8rg>, Brand et al., 2020), nitrate isotope (<https://doi.org/10/fg27>, Tuerena and Ganeshram, 2020) for JR17005 are publicly available from the British Oceanographic Database website. Silicon isotope data will be made publicly available on the British Oceanographic Database website (JR17005) and the Norwegian Polar Institute Data repository (FS2017-FS2919) upon acceptance of the manuscript.

Author contribution. MCFD wrote the manuscript. MCFD, LP, RET, PAD and RSG designed the study. MCFD, RET and AD analysed nitrate isotope samples. MCFD and LP analysed silicon isotope samples. All authors contributed to field work implementation and to the final version of the manuscript.

Competing interests. The authors declare that they have no conflict of interest.

Acknowledgements. We thank the crew and participants of Changing Arctic ocean cruises onboard the RRS James Clark Ross and Fram Strait Arctic Outflow Observatory cruises onboard RV Lance and RV Kronprins Haakon for support in sampling. We also thank the ARISE team for the collaborative sampling effort and sharing scientific ideas.

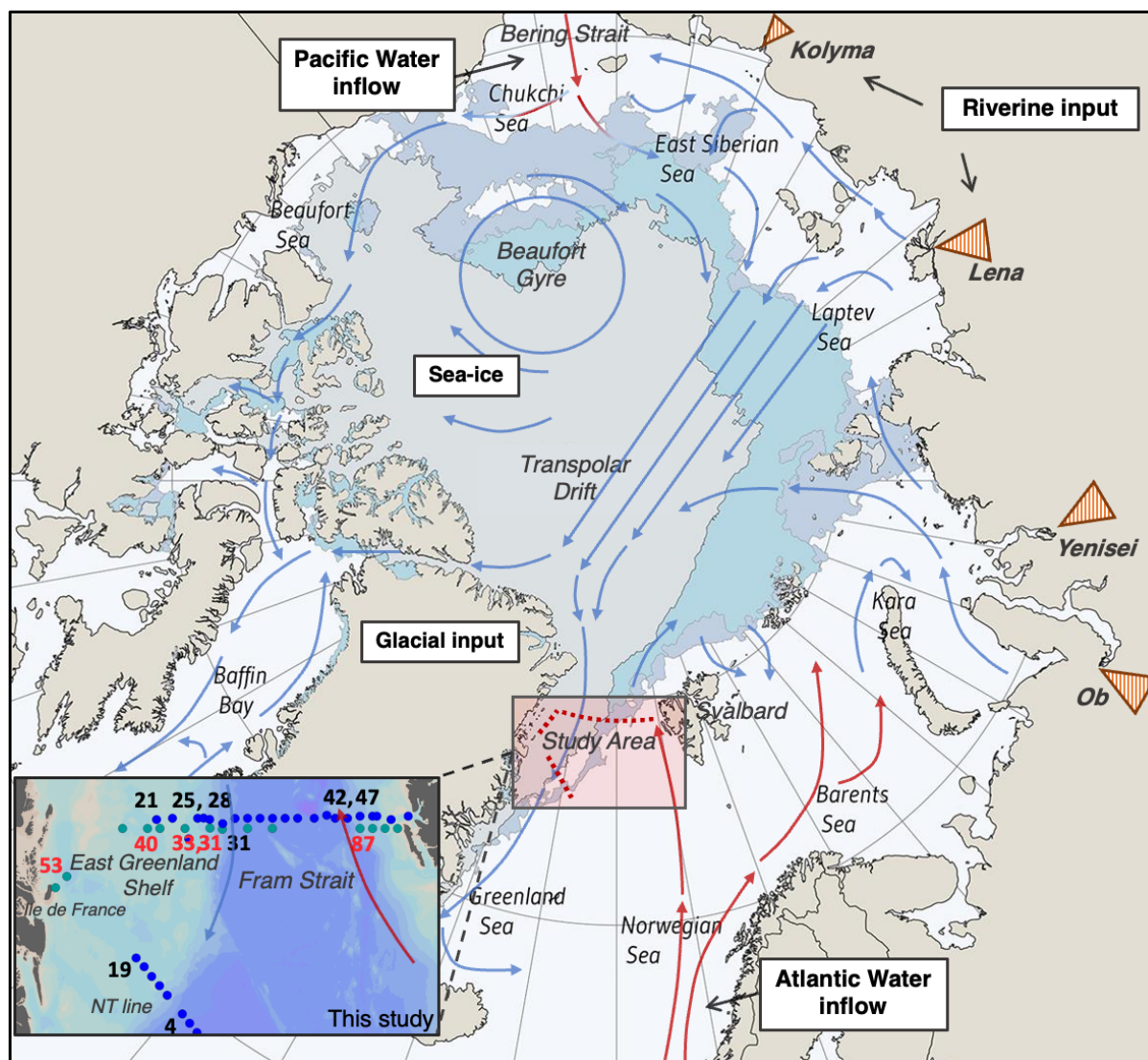


Table 1: Summary of sections along which samples were collected

Year	Cruise	Dates	Vessel	Section Latitude
2018	JR17005	9 May - 9 June	RRS James Clark Ross	79°N
2017	FS2017	24 August -13 September	RV Lance	78° 50'N
2018	FS2018	25 August – 11 September	RV Kronprins Haakon	78° 50'N
2019	FS2019	1 September – 16 September	RV Kronprins Haakon	78° 50'N

Table 2: Averaged water mass signatures of the Fram Strait (a) excluding the mixed layer depth and (b) within the mixed layer in spring (JR17005) and summer (FS2018). Water mass definitions based on (Richter et al., 2018). AW = Atlantic Water, PSW = Polar Surface Water, wPSW = warm PSW, AAW = Arctic Atlantic Water, DW = Deep Water, DSOW = Denmark Strait Overflow Water. N* is defined as $N^* = NO_x - 16 \cdot PO_4$ and Si* is defined as $Si^* = Si(OH)_4 - NO_x$.

	Nitrate (μM)	N*	Si*	$\delta^{15}N-NO_3$ (‰)	$\delta^{18}O-NO_3$ (‰)	$\Delta(15-18)$ (‰)	DSi (μM)	$\delta^{30}Si(OH)_4$ (‰)
AW	12.10	-0.55	-6.73	5.18 ± 0.21	2.33 ± 0.51	2.85	5.42	1.74 ± 0.06
PSW	8.24	-2.36	-1.37	5.44 ± 0.14	1.22 ± 0.91	4.22	6.64	1.85 ± 0.09
wPSW	11.51	-0.50	-5.00	5.09 ± 0.34	2.12 ± 0.77	2.97	6.53	
AAW	11.94	-1.19	-5.26	5.31 ± 0.32	1.92 ± 0.77	3.37	6.63	1.74 ± 0.06
DW	14.02	-0.98	-4.58	5.28 ± 0.17	1.60 ± 0.33	3.68	9.45	1.65 ± 0.13
DSOW	12.37	-0.90	-6.20	5.24 ± 0.20	1.90 ± 0.69	3.33	6.15	1.75 ± 0.08
	Nitrate (μM)	N*	Si*	$\delta^{15}N-NO_3$ (‰)	$\delta^{18}O-NO_3$ (‰)	$\Delta(15-18)$ (‰)	DSi (μM)	$\delta^{30}Si(OH)_4$ (‰)
AW spring	3.83	-2.06	-0.73	8.48 ± 2.3	6.70 ± 3.3	1.78	3.19	2.04 ± 0.37
AW summer	2.71	-1.27	-1.76	6.63 ± 2.0	5.23 ± 3.2	1.39	1.03	
PSW spring	1.50	-5.52	2.73	8.80 ± 1.1	4.63 ± 1.5	4.17	4.27	2.12 ± 0.29
PSW summer	0.19	-6.03	1.06				1.26	



Figure

1: Map of the Arctic ocean showing the study area of this research and general surface circulation patterns within the Arctic ocean. Red arrows represent warm, saline currents of the Atlantic and Pacific, and blue arrows represent fresh, cold water modified within the Arctic ocean (adapted from Tremblay et al., 2005). Orange triangles show the river deltas of four rivers which constitute the largest freshwater source to the Atlantic-Arctic sector: the Ob, Yenisei, Lena & Kolyma rivers. Shaded areas of the central Arctic shows sea ice extant for 2006 (dark blue), 2017 (light blue) and 2020 (grey-blue). Figure adapted from NSIDC, 2020. Inset: Water sample stations for this study are shown with blue dots (JR17005) and green dots (FS2018). Station numbers for silicon isotope profiles measured within this study are shown in red for FS2018 & black for JR17005.

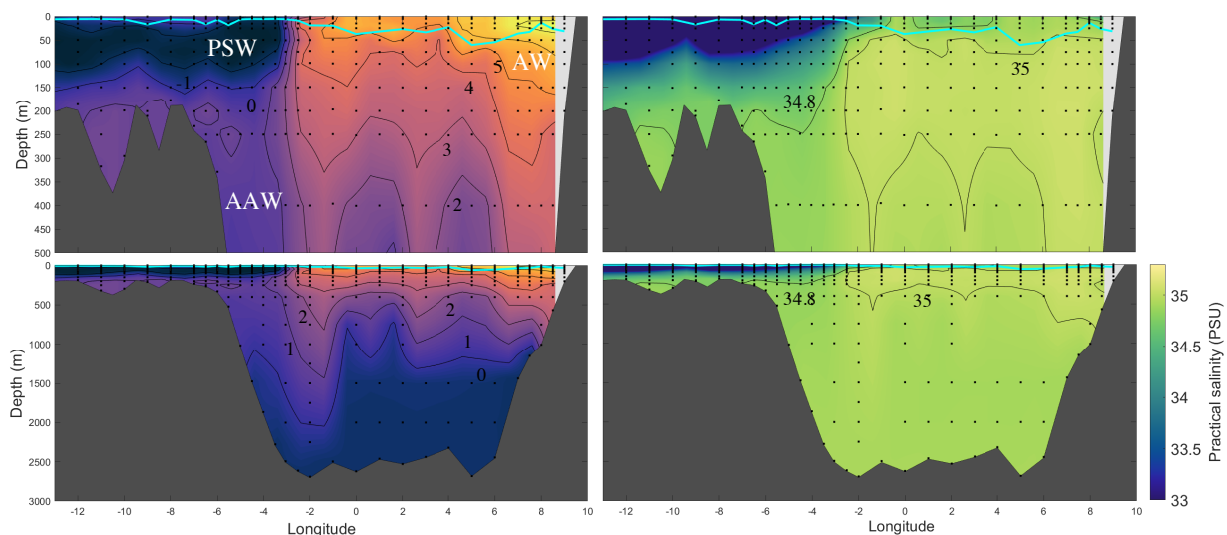


Figure 2: Hydrography of Fram Strait cruise FS2018 from August-September 2018 presented for full depth (bottom panel) and upper water column (top panel). The mixed-layer depth is shown by a cyan line (calculation of MLD is described in method section below). Isotherms (left) & isohalines (right) are also displayed. Atlantic Water (AW), Polar Surface Water (PSW) & Arctic Atlantic Water (AAW) are marked.

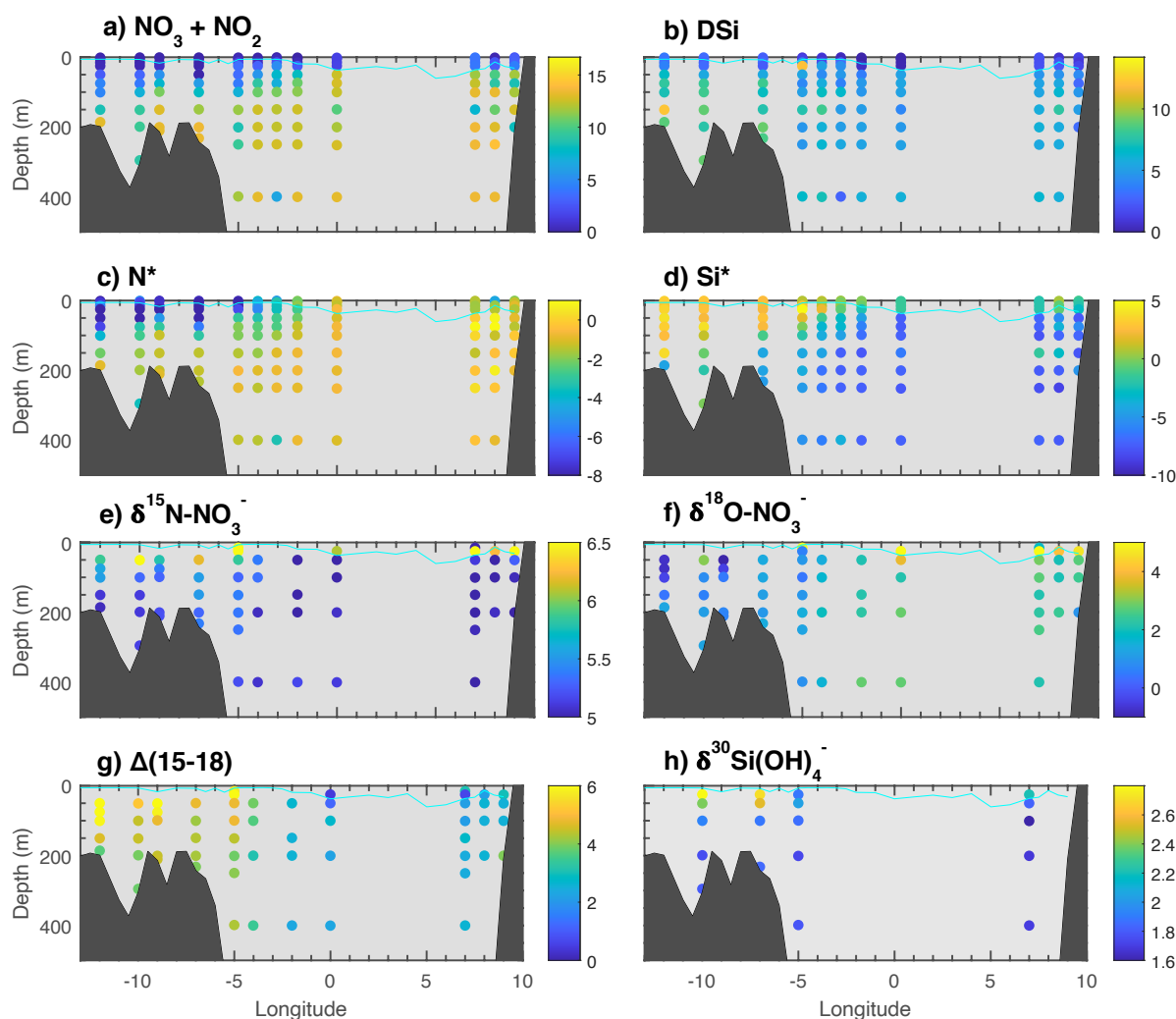


Figure
Figure 3: Nutrients and isotopes across Fram Strait section of 2018 a) NO_x (where NO_x= nitrate + nitrite), b) DSi, c) N^{*} (where N^{*}=
NO_x – 16*PO₄⁻), d) Si^{*} (where Si^{*} = Si(OH)₄ - NO_x), e) δ¹⁵N-NO₃⁻, f) δ¹⁸O-NO₃⁻, g) Δ(15-18) (where Δ(15-18) = δ₁₅N-NO₃⁻ - δ¹⁸O-
NO₃⁻), h) δ³⁰Si(OH)₄⁻. Cyan line displays MLD for the section (calculation described in method section).

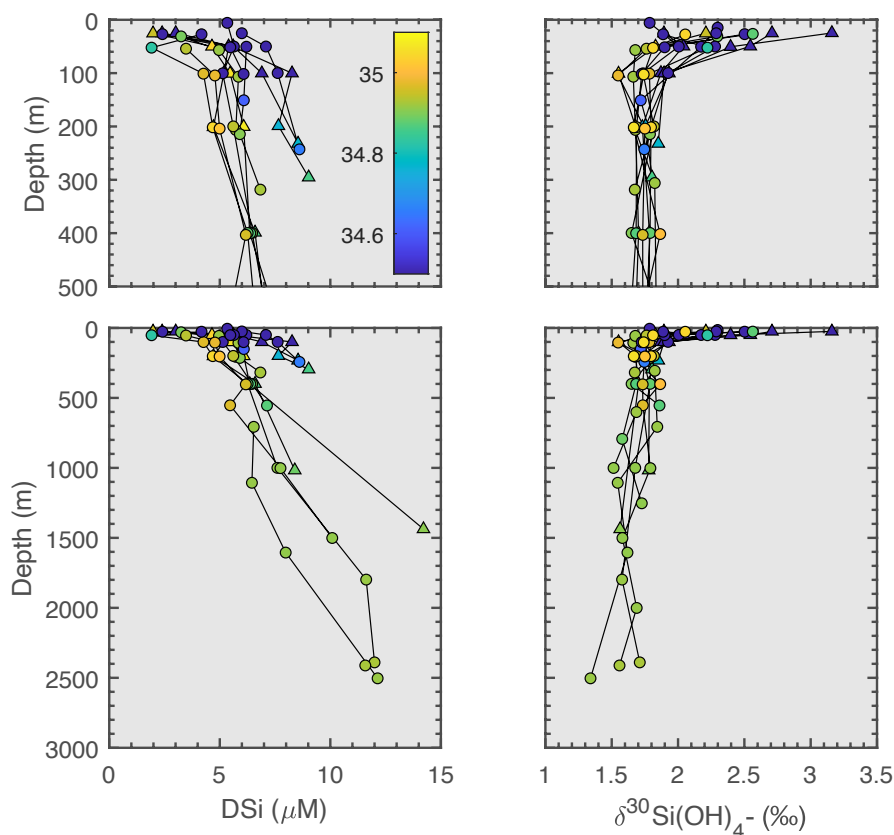


Figure 4: Silica concentrations (left) and dissolved silicon isotope profiles (right) for spring (JR17005, circles) and late summer (FS2018, triangles) of the 2018 growth season in Fram Strait. Colour scale represents salinity (psu).

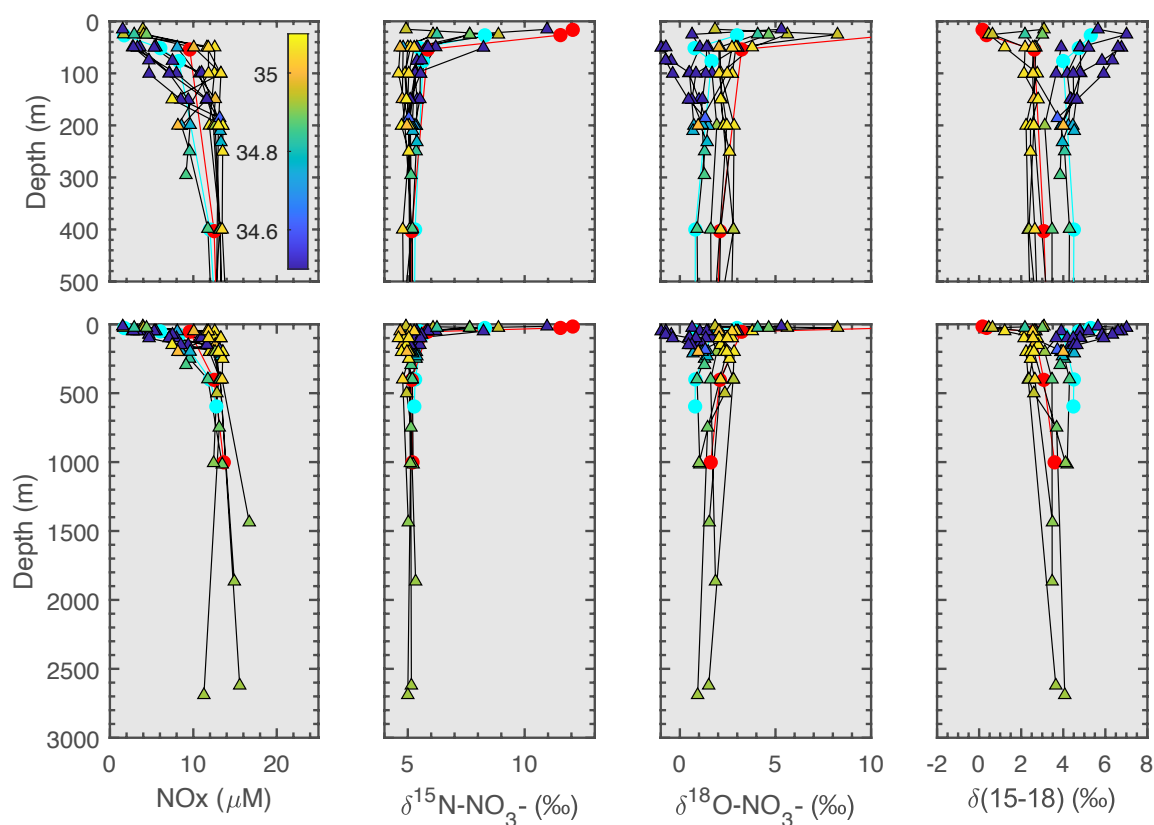


Figure 5: Nitrate concentrations (left), $\delta^{15}\text{N-NO}_3^-$ (middle-left), $\delta^{18}\text{O-NO}_3^-$ (middle-right) and $\Delta(15-18)$ profiles (right) for FS2018 (triangles) in Fram Strait. Typical profiles for PSW (cyan) and AW (red) from JR17005 are shown in circles for comparison between studies (Tuerena et al., 2021). Colourscale represents salinity (psu).

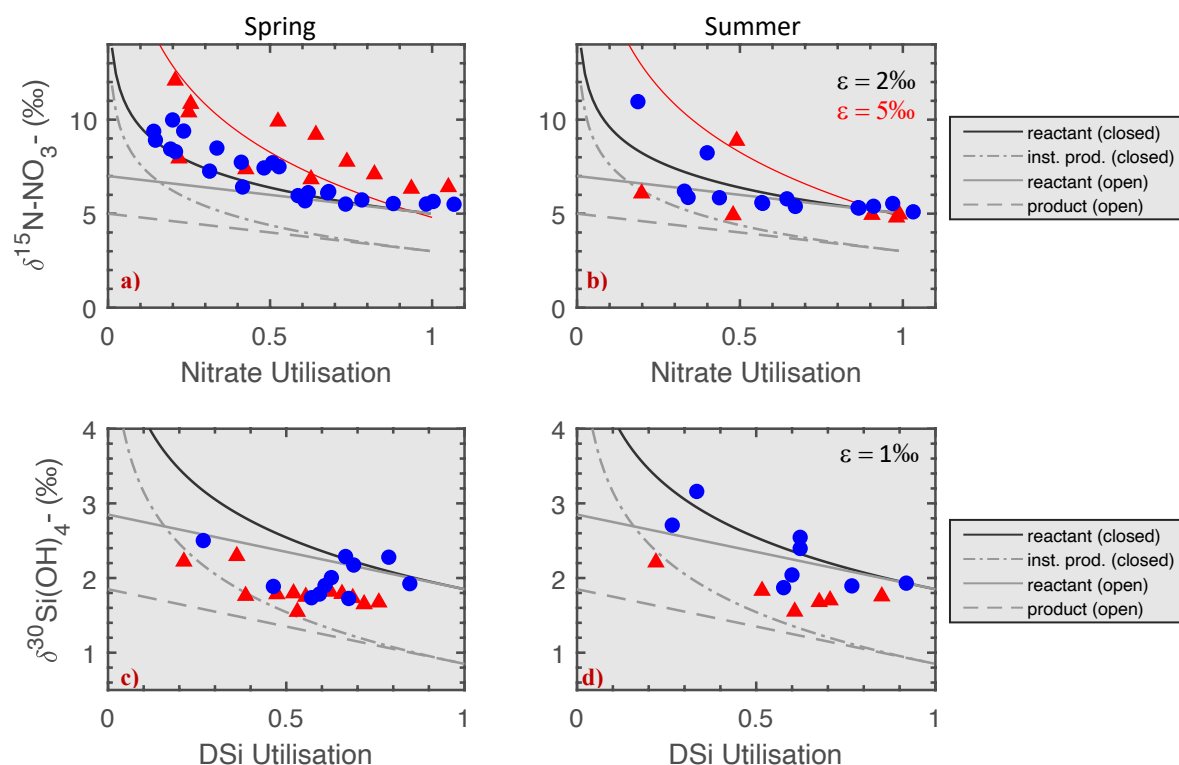


Figure 6: Top panels: nitrate utilisation vs $\delta^{15}\text{N-NO}_3^-$ for spring (left) and summer (right). Black and grey lines describe the fractionation lines for an isotopic effect of 5‰ (AW) and red line for an isotopic effect of 2‰ (PSW). Bottom panels: DSi utilisation vs $\delta^{30}\text{Si(OH)}_4$ for spring (left) and summer (right). Black and grey lines describe the fractionation lines for an isotopic effect of 1‰. Blue circles denote PSW, red triangles denote AW.

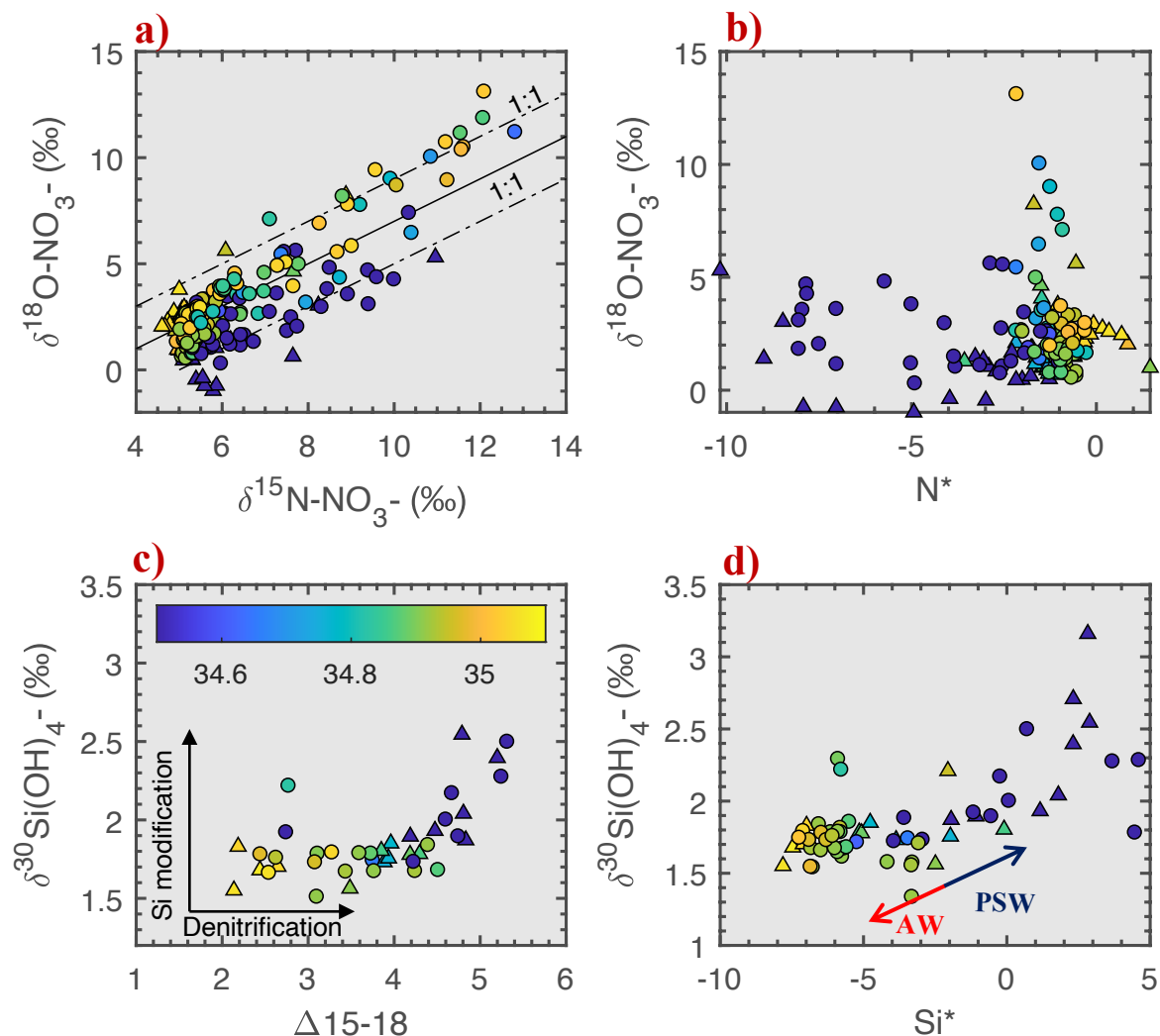


Figure 7: Fram Strait measurements of a) $\delta^{15}\text{N-NO}_3$ vs $\delta^{18}\text{O-NO}_3$ (solid and dotted lines show 1:1 fractionation lines). b) $\delta^{18}\text{O-NO}_3$ vs N^* . c) $\Delta(15-18)$ vs $\delta^{30}\text{Si(OH)}_4$ excluding samples from within the mid-layer depth to remove seasonal variation. d) Si^* vs $\delta^{30}\text{Si(OH)}_4$. In all figures, circles represent spring (JR17005) and triangles show late summer (FS2018). Colorscale for all plots show salinity (psu).

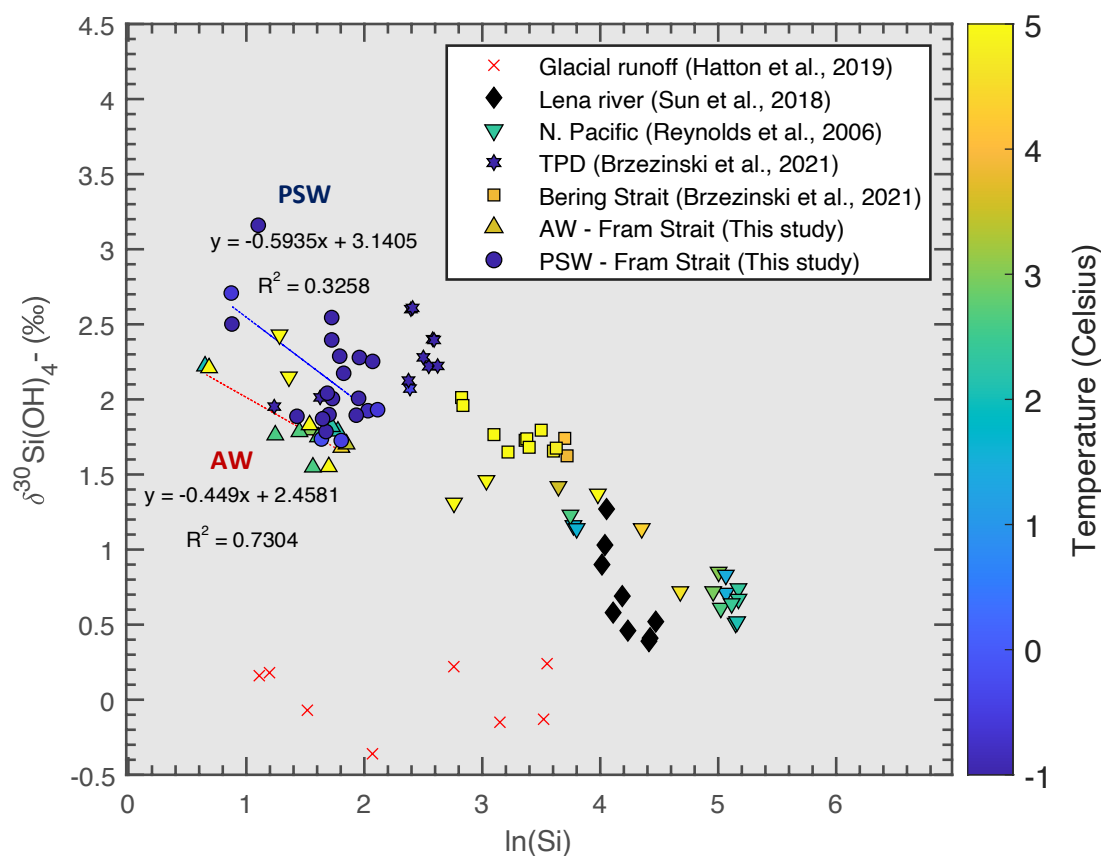


Figure 8: Pan-Arctic trends of $\delta^{30}\text{Si}(\text{OH})_4$ against $\ln(\text{Si})$. Atlantic water at Fram Strait = triangles; red dotted trendline is least-squared regression showing uptake trends in AW. Polar Surface Water at Fram Strait = circles (this study); blue trendline is least-squared regression for the uptake trend in PSW. Cross = Glacial runoff from Greenland and Svalbard glaciers (Hatton et al., 2019); Diamonds = Lena River (Sun et al., 2018); Downward-pointing triangles = North Pacific below the uptake zone (Reynolds et al., 2006); Stars = Transpolar Drift (Brzezinski et al., 2021); Squares = Bering Strait (Brzezinski et al., 2021). Where data is available, colorscale represents temperature (this excludes glacial runoff and Lena River datasets).

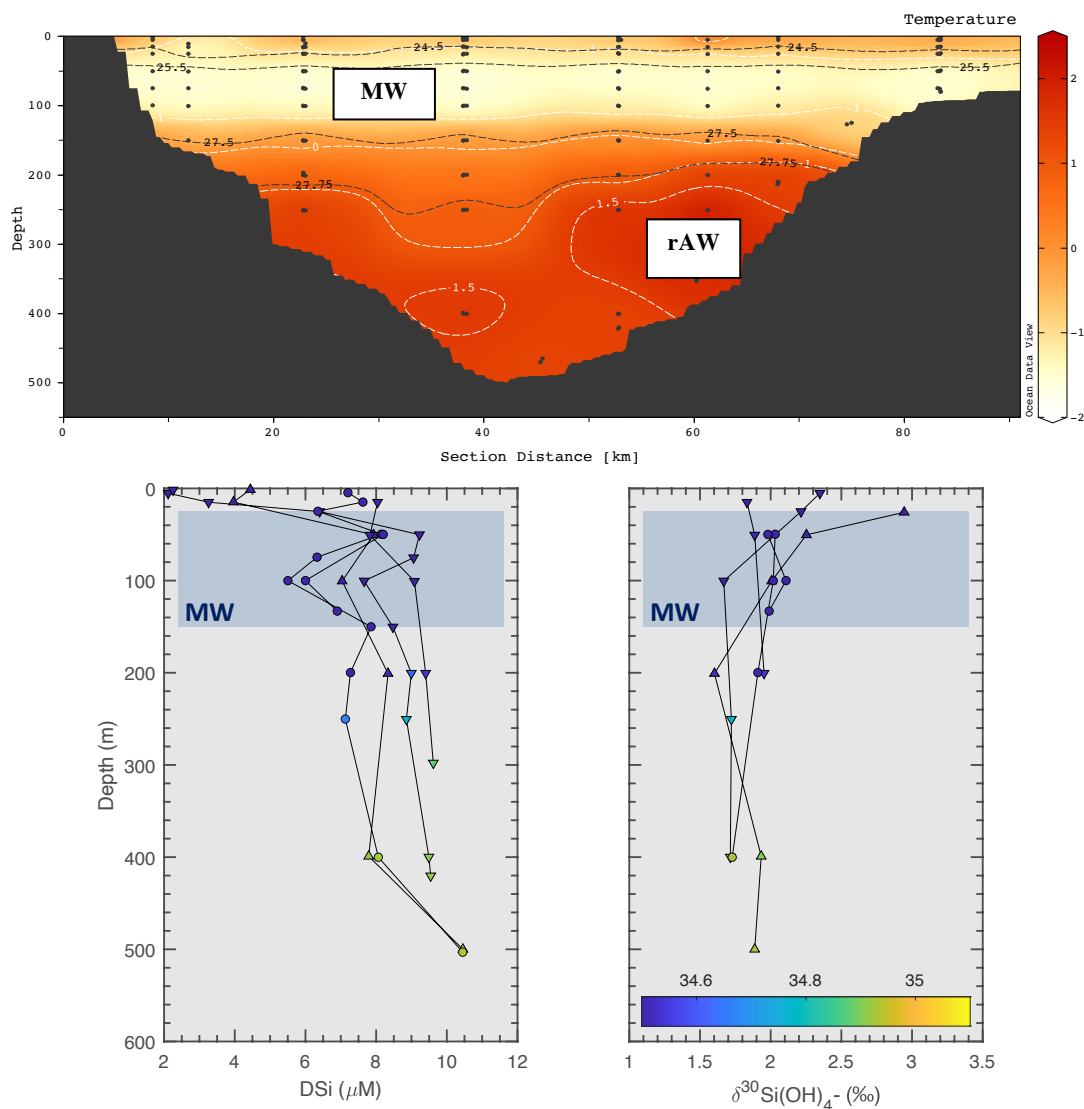


Figure 9: Top: Integrated hydrography of the Ile-de-France section for 2017-2019. Isotherms are shown in white and isopycnals in black. MW = meteoric water, rAW = recirculated Atlantic Water. Bottom panels: Silica concentrations (left) and $\delta^{30}\text{Si}(\text{OH})_4$ (right) for late summer 2017 (circle), 2018 (upwards triangle) & 2019 (downwards triangle) of the Ile-de-France section. Colourscale represents salinity (psu).

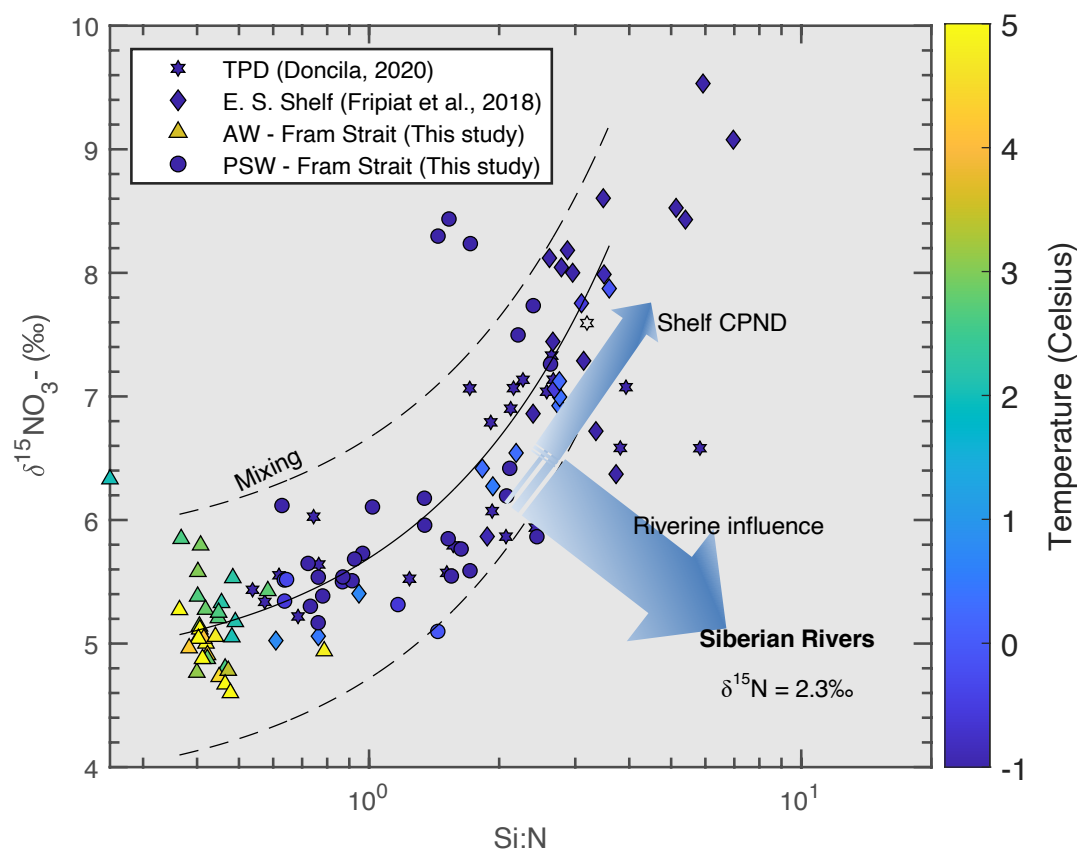


Figure 10: Pan-Arctic trends of $\delta^{15}\text{N-NO}_3$ against Si:N ratio. Triangles = Atlantic water at Fram Strait; Circles = Polar surface water at Fram Strait (this study). Stars = Transpolar drift (Doncila, 2020); Diamonds = East Siberian shelf (Fripiat et al., 2018). Dotted lines shows the regression (conservative mixing line) between AW and shelf endmembers, dotted lines are for one standard deviation. Data is plotted below the mid-layer depth in Fram Strait to remove seasonal variation. This could not be applied to the transpolar drift and East Siberian shelf due to the shallowness of the watermasses. Colorscale shows temperature. $\delta^{15}\text{N-NO}_3$ endmember for summertime Siberian rivers is obtained from Francis (pers. comm.) from ArcticGRO measurements.



References

- 650 Agustí, S., Assmy, P., Duarte, C. M., Wiedmann, I., Marquez, I. A., Fernández-Méndez, M., Kristiansen, S., Krause, J. W. and Wassmann, P.: Biogenic silica production and diatom dynamics in the Svalbard region during spring, *Biogeosciences*, 15(21), 6503–6517, doi:10.5194/bg-15-6503-2018, 2018.
- Allen, J. T., Brown, L., Sanders, R., Moore, C. M., Mustard, A., Fielding, S., Lucas, M., Rixen, M., Savidge, G., Henson, S. and Mayor, D.: Diatom carbon export enhanced by silicate upwelling in the northeast Atlantic, *Nature*, 437(7059), 728–732, doi:10.1038/nature03948, 2005.
- 655 Altabet, M. A. and Francois, R.: Nitrogen isotope biogeochemistry of the Antarctic polar frontal zone at 170°W, *Deep. Res. Part II Top. Stud. Oceanogr.*, 48(19–20), 4247–4273, doi:10.1016/S0967-0645(01)00088-1, 2001.
- Archer, D., Lyle, M., Rodgers, K. and Froelich, P.: What controls opal preservation in tropical deep-sea sediments?, *Paleoceanography*, 8(1), 7–21, 1993.
- Ardyna, M. and Arrigo, K. R.: Phytoplankton dynamics in a changing Arctic Ocean, *Nat. Clim. Chang.*, 10(10), 892–903, doi:10.1038/s41558-020-0905-y, 2020.
- 660 Arrigo, K. R. and van Dijken, G. L.: Continued increases in Arctic Ocean primary production, *Prog. Oceanogr.*, 136, 60–70, doi:10.1016/j.pocean.2015.05.002, 2015.
- Arrigo, K. R., van Dijken, G. and Pabi, S.: Impact of a shrinking Arctic ice cover on marine primary production, *Geophys. Res. Lett.*, 35(19), 1–6, doi:10.1029/2008GL035028, 2008.
- 665 Arthun, M., Eldevik, T., Smedsrud, L. ., Skagseth, Ø. and Ingvaldsen, R. .: Quantifying the Influence of Atlantic Heat on Barents Sea Ice Variability and Retreat *, *J. Clim.*, 25, 4736–4743, doi:10.1175/JCLI-D-11-00466.1, 2012.
- Brown, Z. W., Casciotti, K. L., Pickart, R. S., Swift, J. H. and Arrigo, K. R.: Aspects of the marine nitrogen cycle of the Chukchi Sea shelf and Canada Basin, *Deep. Res. Part II Top. Stud. Oceanogr.*, 118, 73–87, doi:10.1016/j.dsr2.2015.02.009, 2015.
- Brzezinski, M. A. and Jones, J. L.: Coupling of the distribution of silicon isotopes to the meridional overturning circulation of the North Atlantic Ocean, *Deep. Res. Part II Top. Stud. Oceanogr.*, 116, 79–88, doi:10.1016/j.dsr2.2014.11.015, 2015.
- 670 Brzezinski, M. A., Jones, J. L., Barbara, S., Bidle, K. D. and Azam, F.: The balance between silica production and silica dissolution in the sea : Insights from Monterey Bay , California , applied to the global data set, *Limnol. Oceanogr.*, 48(5), 1846–1854, 2003.
- Brzezinski, M. A., Closset, I., Jones, J. L., de Souza, G. F. and Maden, C.: New Constraints on the Physical and Biological Controls on the Silicon Isotopic Composition of the Arctic Ocean, *Front. Mar. Sci.*, 8(August), doi:10.3389/fmars.2021.699762, 2021.
- 675 Budeus, G. and Schneider, W.: On the hydrography of the Northeast Water Polynya, *J. Geophys. Res.*, 100(C3), 4269–4286, doi:10.1029/94JC02349, 1995.
- Cardinal, D., Alleman, L. Y., De Jong, J., Ziegler, K. and André, L.: Isotopic composition of silicon measured by multicollector plasma source mass spectrometry in dry plasma mode, *J. Anal. At. Spectrom.*, 18(3), 213–218, doi:10.1039/b210109b, 2003.
- Cardinal, D., Alleman, L. Y., Dehairs, F., Savoye, N., Trull, T. W. and André, L.: Relevance of silicon isotopes to Si-nutrient utilization and Si-source assessment in Antarctic waters, *Global Biogeochem. Cycles*, 19(2), 1–13, doi:10.1029/2004GB002364, 2005.
- 680 Casciotti, K. L., Sigman, D. M., Hastings, M. G., Bo, J. K. and Hilkert, A.: Measurement of the Oxygen Isotopic Composition of Nitrate in Seawater and Freshwater Using the Denitrifier Method, *Anal. Chem.*, 74(19), 4905–4912, doi:10.1021/ac020113w, 2002.
- Dodd, P. A., Rabe, B., Hansen, E., Falck, E., MacKensen, A., Rohling, E., Stedmon, C. and Kristiansen, S.: The freshwater composition of the Fram Strait outflow derived from a decade of tracer measurements, *J. Geophys. Res. Ocean.*, 117(11), 1–26, doi:10.1029/2012JC008011, 2012.
- 685 Doncila, A.: Nitrogen Cycling in the Warming Arctic Ocean, PhD thesis, Univ. Edinburgh, 2020.



- Ehlert, C., Doering, K., Wallmann, K., Scholz, F., Sommer, S., Grasse, P., Geilert, S. and Frank, M.: Stable silicon isotope signatures of marine pore waters – Biogenic opal dissolution versus authigenic clay mineral formation, *Geochim. Cosmochim. Acta*, 191, 102–117, doi:10.1016/j.gca.2016.07.022, 2016.
- 690 Le Fouest, V., Babin, M. and Tremblay, J. E.: The fate of riverine nutrients on Arctic shelves, *Biogeosciences*, 10(6), 3661–3677, doi:10.5194/bg-10-3661-2013, 2013.
- Frey, K. E. and McClelland, J. W.: Impacts of permafrost degradation on arctic river biogeochemistry, *Hydrol. Process.*, 23(1), 169–182, doi:10.1002/hyp.7196, 2009.
- Frey, K. E., McClelland, J. W., Holmes, R. M. and Smith, L. G.: Impacts of climate warming and permafrost thaw on the riverine transport of nitrogen and phosphorus to the Kara Sea, *J. Geophys. Res. Biogeosciences*, 112(4), 1–10, doi:10.1029/2006JG000369, 2007.
- 695 Fripiat, F., Cardinal, D., Tison, J. L., Worby, A. and André, L.: Diatom-induced silicon isotopic fractionation in Antarctic sea ice, *J. Geophys. Res. Biogeosciences*, 112(2), doi:10.1029/2006JG000244, 2007.
- Fripiat, F., Cavagna, A. J., Savoye, N., Dehairs, F., André, L. and Cardinal, D.: Isotopic constraints on the Si-biogeochemical cycle of the Antarctic Zone in the Kerguelen area (KEOPS), *Mar. Chem.*, 123(1–4), 11–22, doi:10.1016/j.marchem.2010.08.005, 2011a.
- 700 Fripiat, F., Cavagna, A. J., Dehairs, F., Speich, S., André, L. and Cardinal, D.: Silicon pool dynamics and biogenic silica export in the Southern Ocean inferred from Si-isotopes, *Ocean Sci.*, 7(5), 533–547, doi:10.5194/os-7-533-2011, 2011b.
- Fripiat, F., Tison, J. L., André, L., Notz, D. and Delille, B.: Biogenic silica recycling in sea ice inferred from Si-isotopes: Constraints from Arctic winter first-year sea ice, *Biogeochemistry*, 119(1–3), 25–33, doi:10.1007/s10533-013-9911-8, 2014.
- Fripiat, F., Meiners, K. M., Vancoppenolle, M., Papadimitriou, S., Thomas, D. N., Ackley, S. F., Arrigo, K. R., Carnat, G., Cozzi, S., Delille, B., Dieckmann, G. S., Dunbar, R. B., Fransson, A., Kattner, G., Kennedy, H., Lannuzel, D., Munro, D. R., Nomura, D., Rintala, J. M., Schoemann, V., Stefels, J., Steiner, N. and Tison, J. L.: Macro-nutrient concentrations in Antarctic pack ice: Overall patterns and overlooked processes, *Elementa*, 5, doi:10.1525/elementa.217, 2017.
- 705 Fripiat, F., Declercq, M., Sapart, C. J., Anderson, L. G., Bruechert, V., Deman, F., Fonseca-Batista, D., Humborg, C., Roukaerts, A., Semiletov, I. P. and Dehairs, F.: Influence of the bordering shelves on nutrient distribution in the Arctic halocline inferred from water column nitrate isotopes, *Limnol. Oceanogr.*, 63(5), 2154–2170, doi:10.1002/lno.10930, 2018.
- 710 Georg, R. B., Reynolds, B. C., Frank, M. and Halliday, A. N.: New sample preparation techniques for the determination of Si isotopic compositions using MC-ICPMS, *Chem. Geol.*, 235(1–2), 95–104, doi:10.1016/j.chemgeo.2006.06.006, 2006.
- Granger, J., Sigman, D. M., Needoba, J. A. and Harrison, P. J.: Coupled nitrogen and oxygen isotope fractionation of nitrate during assimilation by cultures of marine phytoplankton, *Limnol. Oceanogr.*, 49(5), 1763–1773, doi:10.4319/lo.2004.49.5.1763, 2004.
- 715 Granger, J., Prokopenko, M. G., Sigman, D. M., Mordy, C. W., Morse, Z. M., Morales, L. V., Sambrotto, R. N. and Plessen, B.: Coupled nitrification-denitrification in sediment of the eastern Bering Sea shelf leads to ^{15}N enrichment of fixed N in shelf waters, *J. Geophys. Res. Ocean.*, 116(11), 1–18, doi:10.1029/2010JC006751, 2011.
- Granger, J., Sigman, D. M., Gagnon, J., Tremblay, J. E. and Mucci, A.: On the Properties of the Arctic Halocline and Deep Water Masses of the Canada Basin from Nitrate Isotope Ratios, *J. Geophys. Res. Ocean.*, 123(8), 5443–5458, doi:10.1029/2018JC014110, 2018.
- 720 Grasse, P., Ryabenko, E., Ehlert, C., Altabet, M. A. and Frank, M.: Silicon and nitrogen cycling in the upwelling area off Peru: A dual isotope approach, *Limnol. Oceanogr.*, 61(5), 1661–1676, doi:10.1002/lno.10324, 2016.
- Grasse, P., Brzezinski, M. A., Cardinal, D., Souza, G. F. De, Estrade, N., François, R., Frank, M., Jiang, G., Jones, J. L., Kooijman, E., Liu, Q., Lu, D., Pahnke, K., Ponzevera, E., Schmitt, M., Sun, X., Sutton, J. N., Thil, F. and Weis, D.: GEOTRACES inter-calibration of the stable silicon isotope composition of dissolved silicic acid in seawater, *J. Anal. At. Spectrom.*, 562–578, doi:10.1039/c6ja00302h, 2017.
- 725 Gruber, N. and Sarmiento, J. L.: Global patterns of marine nitrogen fixation and denitrification, *Global Biogeochem. Cycles*, 11(2), 235–266, 1997.



- Hatton, J. E., Hendry, K. R., Hawkings, J. R., Wadham, J. L., Opfergelt, S., Kohler, T. J., Yde, J. C., Stibal, M. and Žárský, J. D.: Silicon isotopes in Arctic and sub-Arctic glacial meltwaters: the role of subglacial weathering in the silicon cycle, *Proc. R. Soc. A Math. Phys. Eng. Sci.*, 475(2228), 20190098, doi:10.1098/rspa.2019.0098, 2019.
- 730 Hátún, H., Azetsu-Scott, K., Somavilla, R., Rey, F., Johnson, C., Mathis, M., Mikolajewicz, U., Coupel, P., Tremblay, J., Hartman, S., Pacariz, S. V., Salter, I. and Ólafsson, J.: The subpolar gyre regulates silicate concentrations in the North Atlantic, *Sci. Rep.*, 7(1), 1–9, doi:10.1038/s41598-017-14837-4, 2017.
- Hawkings, J. R., Wadham, J. L., Benning, L. G., Hendry, K. R., Tranter, M., Tedstone, A., Nienow, P. and Raiswell, R.: Ice sheets as a missing source of silica to the polar oceans, *Nat. Commun.*, 8(May 2016), 1–10, doi:10.1038/ncomms14198, 2017.
- 735 Hawkings, J. R., Hatton, J. E., Hendry, K. R., de Souza, G. F., Wadham, J. L., Ivanovic, R., Kohler, T. J., Stibal, M., Beaton, A., Lamarche-Gagnon, G., Tedstone, A., Hain, M. P., Bagshaw, E., Pike, J. and Tranter, M.: The silicon cycle impacted by past ice sheets, *Nat. Commun.*, 9(1), 1–10, doi:10.1038/s41467-018-05689-1, 2018.
- Henson, S. A., Sanders, R., Holeton, C. and Allen, J. T.: Timing of nutrient depletion, diatom dominance and a lower-boundary estimate of export production for Irminger Basin, North Atlantic, *Mar. Ecol. Prog. Ser.*, 313, 73–84, doi:10.3354/meps313073, 2006.
- 740 Holmes, R. M., McClelland, J. W., Peterson, B. J., Tank, S. E., Bulygina, E., Eglinton, T. I., Gordeev, V. V., Gurtovaya, T. Y., Raymond, P. A., Repeta, D. J., Staples, R., Striegl, R. G., Zhulidov, A. V and Zimov, S. A.: Seasonal and Annual Fluxes of Nutrients and Organic Matter from Large Rivers to the Arctic Ocean and Surrounding Seas, *Estuaries and Coasts*, 35, 369–382, doi:10.1007/s12237-011-9386-6, 2012.
- Holmes, R. M., McClelland, J. W., Tank, S. E., Spencer, R. G. M. and Shiklomanov, A. I.: Arctic Great Rivers Observatory. Water Quality Dataset, (Version 20210608), 2021.
- 745 Hutchins, D. A. and Bruland, K. W.: Iron-limited growth and Si:N ratios in a coastal upwelling regime, *Nature*, 393(June), 561–564, 1998.
- Kamatani, A.: Dissolution rates of silica from diatoms decomposing at various temperatures, *Mar. Biol.*, 68(1), 91–96, doi:10.1007/BF00393146, 1982.
- Karl, D. M. and Tien, G.: MAGIC: A sensitive and precise method for measuring dissolved phosphorus in aquatic environments, *Limnol. Oceanogr.*, 37(1), 105–116, doi:10.4319/lo.1992.37.1.0105, 1992.
- 750 Krause, J. W., Duarte, C. M., Marquez, I. A., Assmy, P., Fernández-Méndez, M., Wiedmann, I., Wassmann, P., Kristiansen, S. and Agustí, S.: Biogenic silica production and diatom dynamics in the Svalbard region during spring, *Biogeosciences Discuss.*, 2(May), 1–25, doi:10.5194/bg-2018-226, 2018.
- Krause, J. W., Schulz, I. K., Rowe, K. A., Dobbins, W., Winding, M. H. S., Sejr, M. K., Duarte, C. M. and Agustí, S.: Silicic acid limitation drives bloom termination and potential carbon sequestration in an Arctic bloom, *Sci. Rep.*, 9(1), 1–11, doi:10.1038/s41598-019-44587-4, 2019.
- 755 Krisch, S., Browning, T. J., Graeve, M., Ludwichowski, K. U., Lodeiro, P., Hopwood, M. J., Roig, S., Yong, J. C., Kanzow, T. and Achterberg, E. P.: The influence of Arctic Fe and Atlantic fixed N on summertime primary production in Fram Strait, North Greenland Sea, *Sci. Rep.*, 10(1), 1–13, doi:10.1038/s41598-020-72100-9, 2020.
- Lalande, C., Bauerfeind, E., Nöthig, E. M. and Beszczynska-Möller, A.: Impact of a warm anomaly on export fluxes of biogenic matter in the eastern Fram Strait, *Prog. Oceanogr.*, 109, 70–77, doi:10.1016/j.pocean.2012.09.006, 2013.
- 760 Leblanc, K., Leynaert, A., Fernandez, I. C., Rimmelin, P., Moutin, T., Raimbault, P., Ras, J. and Quéguiner, B.: A seasonal study of diatom dynamics in the North Atlantic during the POMME experiment (2001): Evidence for Si limitation of the spring bloom, *J. Geophys. Res. C Ocean.*, 110(7), 1–16, doi:10.1029/2004JC002621, 2005.
- Letscher, R. T., Hansell, D. A., Kadko, D. and Bates, N. R.: Dissolved organic nitrogen dynamics in the Arctic Ocean, *Mar. Chem.*, 148, 1–9, doi:10.1016/j.marchem.2012.10.002, 2013.
- 765 Liguori, B. T. P., Ehlert, C. and Pahnke, K.: The Influence of Water Mass Mixing and Particle Dissolution on the Silicon Cycle in the Central Arctic Ocean, *Front. Mar. Sci.*, 7(April), 1–16, doi:10.3389/fmars.2020.00202, 2020.



Lind, S., Ingvaldsen, R. B. and Furevik, T.: Arctic warming hotspot in the northern Barents Sea linked to declining sea-ice import, *Nat. Clim. Chang.*, 8(634), doi:10.1038/s41558-018-0205-y, 2018.

770 Mariotti, A., Germon, J. C., Hubert, P., Kaiser, P., Letolle, R., Tardieu, A. and Tardieu, P.: Experimental determination of nitrogen kinetic isotope fractionation: some principles; illustration for the denitrification and nitrification processes, *Plant Soil*, 62, 413–430, 1981.

Mavromatis, V., Rinder, T., Prokushkin, A. S., Pokrovsky, O. S., Korets, M. A., Chmeleff, J. and Oelkers, E. H.: The effect of permafrost, vegetation, and lithology on Mg and Si isotope composition of the Yenisey River and its tributaries at the end of the spring flood, *Geochim. Cosmochim. Acta*, 191, 32–46, doi:10.1016/j.gca.2016.07.003, 2016.

775 Mcclelland, J. W., De, S. J., Peterson, B. J., Holmes, R. M. and Wood, E. F.: A pan-arctic evaluation of changes in river discharge during the latter half of the 20th century, *Geophys. Res. Lett.*, 33, 2–5, doi:10.1029/2006GL025753, 2006.

Mctigue, N. D., Gardner, W. S., Dunton, K. H. and Hardison, A. K.: Biotic and abiotic controls on co-occurring nitrogen cycling processes in shallow Arctic shelf sediments, *Nat. Commun.*, 7, 1–11, doi:10.1038/ncomms13145, 2016.

780 Moore, C. M., Mills, M. M., Arrigo, K. R., Berman-Frank, I., Bopp, L., Boyd, P. W., Galbraith, E. D., Geider, R. J., Guieu, C., Jaccard, S. L., Jickells, T. D., La Roche, J., Lenton, T. M., Mahowald, N. M., Marañón, E., Marinov, I., Moore, J. K., Nakatsuka, T., Oschlies, A., Saito, M. A., Thingstad, T. F., Tsuda, A. and Ulloa, O.: Processes and patterns of oceanic nutrient limitation, *Nat. Geosci.*, 6(9), 701–710, doi:10.1038/ngeo1765, 2013.

785 Nelson, D. M., Tréguer, P., Brzezinski, M. A., Leynaert, A. and Quéguiner, B.: Production and dissolution of biogenic silica in the ocean: Revised global estimates, comparison with regional data and relationship to biogenic sedimentation, *Global Biogeochem. Cycles*, 9(3), 359–372, doi:10.1029/95GB01070, 1995.

Peralta-Ferriz, C. and Woodgate, R. A.: Seasonal and interannual variability of pan-Arctic surface mixed layer properties from 1979 to 2012 from hydrographic data, and the dominance of stratification for multiyear mixed layer depth shoaling, *Prog. Oceanogr.*, 134, 19–53, doi:10.1016/j.pocean.2014.12.005, 2015.

790 Pokrovsky, O. S., Reynolds, B. C., Prokushkin, A. S., Schott, J. and Viers, J.: Silicon isotope variations in Central Siberian rivers during basalt weathering in permafrost-dominated larch forests, *Chem. Geol.*, 355, 103–116, doi:10.1016/j.chemgeo.2013.07.016, 2013.

Popova, E. E., Yool, A., Coward, A. C., Dupont, F., Deal, C., Elliott, S., Hunke, E., Jin, M., Steele, M. and Zhang, J.: What controls primary production in the Arctic Ocean? Results from an intercomparison of five general circulation models with biogeochemistry, *J. Geophys. Res. Ocean.*, 117(1), 1–16, doi:10.1029/2011JC007112, 2012.

795 Rafter, P. A., Difiore, P. J. and Sigman, D. M.: Coupled nitrate nitrogen and oxygen isotopes and organic matter remineralization in the Southern and Pacific Oceans, *J. Geophys. Res. Ocean.*, 118(10), 4781–4794, doi:10.1002/jgrc.20316, 2013.

Randelhoff, A., Reigstad, M., Chierici, M., Sundfjord, A., Ivanov, V., Cape, M., Vernet, M., Tremblay, J.-É., Bratbak, G. and Kristiansen, S.: Seasonality of the Physical and Biogeochemical Hydrography in the Inflow to the Arctic Ocean Through Fram Strait, *Front. Mar. Sci.*, 5(June), 1–16, doi:10.3389/fmars.2018.00224, 2018.

800 Rawlins, M. A., Steele, M., Holland, M. M., Adam, J. C., Cherry, J. E., Francis, J. A., Groisman, P. Y., Hinzman, L. D., Huntington, T. G., Kane, D. L., Kimball, J. S., Kwok, R., Lammers, R. B., Lee, C. M., Lettenmaier, D. P., McDonald, K. C., Podest, E., Pundsack, J. W., Rudels, B., Serreze, M. C., Shiklomanov, A., Skagseth, Ø., Troy, T. J., Vörösmarty, C. J., Wensnahan, M., Wood, E. F., Woodgate, R., Yang, D., Zhang, K. and Zhang, T.: Analysis of the Arctic system for freshwater cycle intensification: Observations and expectations, *J. Clim.*, 23(21), 5715–5737, doi:10.1175/2010JCLI3421.1, 2010.

805 Reynolds, B. C., Frank, M. and Halliday, A. N.: Silicon isotope fractionation during nutrient utilization in the North Pacific, *Earth Planet. Sci. Lett.*, 244(1–2), 431–443, doi:10.1016/j.epsl.2006.02.002, 2006.

Reynolds, B. C., Aggarwal, J., Andre, L., Georg, R. B., Beucher, C., Brzezinski, M. A., Engstro, E., Land, M., Leng, M. J., Opfergelt, S., Rodushkin, I., Sloane, H. J., Boorn, S. H. J. M. Van Den and Vroon, Z.: An inter-laboratory comparison of Si isotope reference materials, *J. Anal. At. Spectrom.*, 22, 561–568, doi:10.1039/b616755a, 2007.

Richter, M. E., Von Appen, W. J. and Wekerle, C.: Does the East Greenland Current exist in the northern Fram Strait?, *Ocean Sci.*, 14(5),



810 1147–1165, doi:10.5194/os-14-1147-2018, 2018.

Rudels, B., Fahrbach, E., Meincke, J., Budéus, G. and Eriksson, P.: The East Greenland Current and its contribution to the Denmark Strait overflow, *ICES J. Mar. Sci.*, 59(6), 1133–1154, doi:10.1006/jmsc.2002.1284, 2002.

815 Rudels, B., Björk, G., Nilsson, J., Winsor, P., Lake, I. and Nohr, C.: The interaction between waters from the Arctic Ocean and the Nordic Seas north of Fram Strait and along the East Greenland Current: Results from the Arctic Ocean-02 Oden expedition, *J. Mar. Syst.*, 55(1–2), 1–30, doi:10.1016/j.jmarsys.2004.06.008, 2005.

Sanders, T., Fiencke, C., Fuchs, M., Haugk, C., Juhls, B., Mollenhauer, G., Ogneva, O., Overduin, P., Palmtag, J., Povazhniy, V., Strauss, J., Tuerena, R., Zell, N. and Dähnke, K.: Seasonal nitrogen fluxes of the Lena River Delta, *Ambio*, 423–438, doi:10.1007/s13280-021-01665-0, 2021.

820 Sarmiento, J. L., Gruber, N., Brzezinski, M. A. and Dunne, J. P.: High-latitude controls of thermocline nutrients and low latitude biological productivity, *Nature*, 427(January), 56–60, doi:10.1038/nature02204.1., 2004.

Schneider, W. and Budeus, G.: On the generation of the Northeast Water Polynya, *J. Geophys. Res.*, 100(C3), 4269–4286, doi:10.1029/94JC02349, 1995.

Sigman, D. M., Altabet, M. A., McCorkle, D. C., Francois, R. and Fischer, G.: The $\delta^{15}\text{N}$ of nitrate in the Southern Ocean: Nitrogen cycling and circulation in the ocean interior, *J. Geophys. Res. Ocean.*, 105(C8), 19599–19614, doi:10.1029/2000JC000265, 2000.

825 Sigman, D. M., Casciotti, K. L., Andreani, M., Barford, C., Galanter, M. and Böhlke, J. K.: A bacterial method for the nitrogen isotopic analysis of nitrate in seawater and freshwater, *Anal. Chem.*, 73(17), 4145–4153, doi:10.1021/ac010088e, 2001.

Sigman, D. M., Granger, J., DiFiore, P. J., Lehmann, M. M., Ho, R., Cane, G. and van Geen, A.: Coupled nitrogen and oxygen isotope measurements of nitrate along the eastern North Pacific margin, *Global Biogeochem. Cycles*, 19(4), 1–14, doi:10.1029/2005GB002458, 2005.

830 De Souza, G. F., Reynolds, B. C., Rickli, J., Frank, M., Saito, M. A., Gerringa, L. J. A. and Bourdon, B.: Southern Ocean control of silicon stable isotope distribution in the deep Atlantic Ocean, *Global Biogeochem. Cycles*, 26(2), 1–13, doi:10.1029/2011GB004141, 2012.

Stedmon, C. A., Granskog, M. A. and Dodd, P. A.: An approach to estimate the freshwater contribution from glacial melt and precipitation in East Greenland shelf waters using colored dissolved organic matter (CDOM), *J. Geophys. Res. Ocean.*, 1107–1117, doi:10.1002/2015JC011107.Received, 2015.

835 de Steur, L., Hansen, E., Gerdes, R., Karcher, M., Fahrbach, E. and Holfort, J.: Freshwater fluxes in the East Greenland Current: A decade of observations, *Geophys. Res. Lett.*, 36(23), L23611, doi:10.1029/2009GL041278, 2009.

Sun, X., Mörrh, C. M., Porcelli, D., Kutscher, L., Hirst, C., Murphy, M. J., Maximov, T., Petrov, R. E., Humborg, C., Schmitt, M. and Andersson, P. S.: Stable silicon isotopic compositions of the Lena River and its tributaries: Implications for silicon delivery to the Arctic Ocean, *Geochim. Cosmochim. Acta*, 241, 120–133, doi:10.1016/j.gca.2018.08.044, 2018.

840 Sutton, J. N., de Souza, G. F., Garcia-Ibáñez, M. I. and De La Rocha, C. L.: The silicon stable isotope distribution along the GEOVIDE section (GEOTRACES GA-01) of the North Atlantic Ocean, *Biogeosciences*, 15, 5663–5676, doi:10.5194/bg-15-5663-2018, 2018.

Terhaar, J., Lauerwald, R., Regnier, P., Gruber, N. and Bopp, L.: Around one third of current Arctic Ocean primary production sustained by rivers and coastal erosion, *Nat. Commun.*, 12(1), 1–10, doi:10.1038/s41467-020-20470-z, 2021.

845 Thibodeau, B., Bauch, D. and Voss, M.: Nitrogen dynamic in Eurasian coastal Arctic ecosystem: Insight from nitrogen isotope, *Global Biogeochem. Cycles*, 31(5), 836–849, doi:10.1002/2016GB005593, 2017.

Torres-Valdés, S., Tsubouchi, T., Bacon, S., Naveira-Garabato, A. C., Sanders, R., McLaughlin, F. A., Petrie, B., Kattner, G., Azetsu-Scott, K. and Whitledge, T. E.: Export of nutrients from the Arctic Ocean, *J. Geophys. Res. Ocean.*, 118(4), 1625–1644, doi:10.1002/jgrc.20063, 2013.

Tremblay, J. É., Anderson, L. G., Matrai, P., Coupel, P., Bélanger, S., Michel, C. and Reigstad, M.: Global and regional drivers of nutrient



- 850 supply, primary production and CO₂ drawdown in the changing Arctic Ocean, *Prog. Oceanogr.*, 139, 171–196, doi:10.1016/j.pocean.2015.08.009, 2015.
- Tuerena, R. E., Ganeshram, R. S., Geibert, W., Fallick, A. E., Dougans, J., Tait, A., Henley, S. F. and Woodward, E. M. S.: Nutrient cycling in the Atlantic basin: The evolution of nitrate isotope signatures in water masses, *Global Biogeochem. Cycles*, 29, 1830–1844, doi:10.1002/2015GB005164, 2015.
- 855 Tuerena, R. E., Hopkins, J., Buchanan, P. J., Ganeshram, R. S., Norman, L., W-Jvon-Appen, Tagliabue, A., Doncila, A., Graeve, M., Ludwichowski, K., Dodd, P. A., Vega, C. de la, Salter, I. and Mahaffey, C.: An Arctic strait of two halves: The changing dynamics of nutrient uptake and limitation across the Fram Strait, *Global Biogeochem. Cycles*, doi:10.1029/2021gb006961, 2021a.
- Tuerena, R. E., Hopkins, J., Ganeshram, R. ., Norman, L., De La Vega, C., Jeffreys, R. and Mahaffey, C.: Nitrate assimilation and regeneration in the Barents Sea: Insights from nitrate isotopes, *Biogeosciences*, 18(2), 637–653, doi:10.5194/bg-18-637-2021, 2021b.
- 860 Tuerena, R. E., Mahaffey, C., Henley, S. F., de la Vega, C., Norman, L., Brand, T., Sanders, T., Debyser, M., Dähnke, K., Braun, J. and März, C.: Nutrient pathways and their susceptibility to past and future change in the Eurasian Arctic Ocean, *Ambio*, 355–369, doi:10.1007/s13280-021-01673-0, 2021c.
- Varela, D. ., Brzezinski, M. ., Beucher, C. ., Jones, J. ., Giesbrecht, K. ., Lansard, B. and Mucci, A.: Heavy silicon isotopic composition of silicic acid and biogenic silica in Arctic waters over the Beaufort shelf and the Canada Basin, *Global Biogeochem. Cycles*, 30, 804–824, doi:10.1002/2015GB005277, Received, 2016.
- 865 Varela, D. E., Pride, C. J. and Brzezinski, M. A.: Biological fractionation of silicon isotopes in Southern Ocean surface waters, *Global Biogeochem. Cycles*, 18(1), n/a–n/a, doi:10.1029/2003GB002140, 2004.
- Weigand, M. A., Foriel, J., Barnett, B., Oleynik, S. and Sigman, D. M.: Updates to instrumentation and protocols for isotopic analysis of nitrate by the denitrifier method, *Rapid Commun. Mass Spectrom.*, 30(12), 1365–1383, doi:10.1002/rcm.7570, 2016.
- 870 Woodgate, R. A.: Increases in the Pacific inflow to the Arctic from 1990 to 2015, and insights into seasonal trends and driving mechanisms from year-round Bering Strait mooring data, *Prog. Oceanogr.*, 160(June 2017), 124–154, doi:10.1016/j.pocean.2017.12.007, 2018.
- Yamamoto-Kawai, M., Carmack, E. and McLaughlin, F.: Nitrogen balance and Arctic throughflow, *Nature*, 443(7107), 43, doi:10.1038/443043a, 2006.
- Yool, A., Popova, E. E. and Coward, A. C.: Future change in ocean productivity: Is the Arctic the new Atlantic, *J. Geophys. Res. Ocean.*, 120(12), 7771–7790, doi:10.1002/2015JC011167, 2015.
- 875 Young, E. D., Galy, A. and Nagahara, H.: Kinetic and equilibrium mass-dependent isotope fractionation laws in nature and their geochemical and cosmochemical significance, *Geochim. Cosmochim. Acta*, 66(6), 1095–1104, doi:10.1016/S0016-7037(01)00832-8, 2002.
- Zhang, S. M., Mu, C. C., Li, Z. L., Dong, W. W., Wang, X. Y., Streletskaia, I., Grebenets, V., Sokratov, S., Kizyakov, A. and Wu, X. D.: Export of nutrients and suspended solids from major Arctic rivers and their response to permafrost degradation, *Adv. Clim. Chang. Res.*, 12(4), 466–474, doi:10.1016/j.accre.2021.06.002, 2021.
- 880